Assessment of hepatoprotective, renal protective and anti-genotoxic effect of novel synthesized complexes of Ca(II), Mg(II) and Cr(III) with 2,6-dichloroindophenol against Acrylamide toxicity in male rats

Refat Moamen S.[1,2*], Hamza Reham Z.[3,4], Adam A.M.A.[1], Saad H.A.[1,5], Gobouri Adil A.[1], Al-Salmi Fawziah A.[3], Altalhi T.[1] and El-Megharbel Samy M.[1,5]

1. Department of Chemistry, Faculty of Science, Taif University, Main campus, P.O. Box 888, Zip Code 21974, Taif, SAUDI ARABIA
2. Department of Chemistry, Faculty of Science, Port Said University, Port Said, EGYPT
3. Biology Department, Faculty of Science, Taif University, Taif, Main campus, P.O. Box 888, Zip Code 21974, SAUDI ARABIA
4. Zoology Department, Faculty of Science, Zagazig University, Zagazig 44519, EGYPT
5. Department of Chemistry, Faculty of Science, Zagazig University 44519, EGYPT
*msrefat@yahoo.com

Abstract

Herein this study aimed to prepare and spectroscopically investigate magnesium(II), calcium(II) and chromium(III) complexes with 2,6-dichloroindo phenol sodium hydrate (Dich). The suggestion formula can be presented as $[Mg(Dich)_2(H_2O)_4].5H_2O$, $[Ca(Dich)_2(H_2O)_4].2H_2O$ and $[Cr(Dich)_3(H_2O)_3].3H_2O$ according to micro analytical, conductivity, FTIR, magnetic susceptibility, UV–Visible, TG-DrTGA, SEM and TEM studies. The analyses revealed that the Dich ligand acts as a monodentate chelating through the oxygen atom of –OH phenolic group with an octahedral geometry around the central metal ions. The six–coordination sphere was completing by coordinated water molecules. This study aimed to evaluate the potent antioxidant, antihepatorenal toxicity and antigenotoxic effects of acrylamide (AC) and role of the novel complexes Ca/Dich, Mg/Dich and Cr/Dich in alleviating hepatorenaltoxicity, oxidative injury and genotoxicity induced by AC in male albino rats. After 30 consecutive days of exposure, some biochemical parameters were measured as hepatic aminotransferases enzymes, lipid profile, kidney function parameters, TNF-α, IL-6, markers of inflammation, tissue damage LDH, CRP, mitochondrial potential activities, MPO, XO, CRP,SDH , MMP , MDA levels and antioxidant enzymes (SOD , CAT , GRx and GST) ,ATP content with histological, TEM examination of the hepatic and renal tissues and Alkaline comet assay in hepatic tissues .

AC induced biochemical and cellular alterations in the hepatic and renal tissues and theses toxicity were alleviated greatly after treatment of male rats with the novel complexes Ca/Dich, Mg/Dich and Cr/Dich which afforded protection against hepatorenal injury and oxidative stress resulting from AC toxicity. Consequently, the novel complexes improved the hepatic enzymes and improved the antioxidant capacities in the hepatic and renal tissues.

Keywords: Dichloroindophenol, Acrylamide, Complexity, Mg^{II}, Ca^{II}, Cr^{III}, Genotoxicity, COVID-19.

Introduction

Liver plays a vital and potent key role in the excretion and metabolism of a lot of xenobiotics which makes it very sensitive to the xenobiotics high toxic effects. Liver damage caused by different toxic chemicals (hepatotoxicants) is known as hepatotoxicity, Thus, the hepatotoxicity may refer to the liver dysfunction or hepatic injury which is associated with an overload of xenobiotics or drugs[1]. Acrylamide (ACR) is a water soluble compound. ACR is mainly formed in the fried potatoes as sort of starchy foods that are heated over 120°C for long periods[1].

Acrylamide (ACR) is widely used industrially in synthesis of the dyes and cosmetic manufacturing[2]. ACR is formed in foods rich with carbohydrate that were heated higher than 120°C[3]. ACR is formed due to cooking at high temperatures by interaction between amino acid asparagine and a carbonyl[4]. The benzene chloride compounds are small types of cyclic hydrocarbon aromatic compounds which are produced by the substitution of chlorine with a single phenyl ring[1]. 2,6-Dichloroindophenol is a dye which acts as a pH oxidation and reduction indicator for different applications[2].

Dichlorobenzene is used for the synthesis of organics, manufacturing of dye and it is used as a solvent in the chemical industry[3]. A lot of drugs may induce hepatic injury when administrated even with the adjusted therapeutic doses. Hepatic toxicity may result from reactive metabolites or from the mediated immunologically-response affecting the hepatic cells or liver cellular structure[4,5]. The hepatotoxic response elicited by a chemical agents depends on the concentration of the toxicant which may be toxic metabolites and concentration gradient of cofactors in the blood[6].

Hepatotoxic response is expressed in the form of many characteristic patterns and may induce severe abdominal pain, nausea or vomiting, weakness, light colored stool and

sometimes the dark urine[7,8]. Liver is the largest organ of the human body weighing about 1,5 kg and is located in the upper right corner of the abdomen. Liver performs more than 500 vital metabolic functions[9].

Hepatic parenchyma acts as a storage organ for a lot of products such as glycogen and some vitamins. Liver is also responsible for the production of the bile. Bile helps in the removal of toxic substances and serves as a filter that separates out harmful substances from the bloodstream[4]. Endoplasmic reticulum (RE) is the major "metabolic clearing house" of the liver for a lot of endogenous chemicals such as cholesterol, steroid hormones, fatty acids and proteins and exogenous substances such as drugs.

The major role of the liver is the transformation of toxic damage of some chemicals and manages them[4]. Calcium and magnesium have great protective and hepatoprotective effects against many xenobiotics and pollutants and may compete for receptors in the cells.

Dabak et al[10] have shown that calcium and magnesium have potent protective effects against the hepatotoxicity of both cadmium (Cd) and lead (Pb). Nutrition plays a vital role in the development and in the prevention of lot of diseases such as cancer, cardiovascular diseases and diabetes. Chromium (Cr) is considered as one of the trace elements which are necessary for normal functioning of the cells' vitality[11].

COVID-19 was considered as a pandemic according to WHO in March 2020, it causes several body organs toxicity in vital organs like liver and kidney and thus the novel complexes in the current study (Ca/Dich, Mg/Dich and Cr/Dich) can be a new hope for disinfecting the virus to offer protection against COVID-19. So, purpose of the current study was to evaluate the antioxidant, anti-inflammatory and anti-genotoxicity effects of novel complexes (Ca/Dich, Mg/Dich and Cr/Dich) in alleviating ROS, genotoxicity and hepatotoxicity induced by AC by using the rat model experiment.

Material and Methods

Chemical and analyses: All chemicals were of reagent grade. 2,6-dichloroindophenol sodium salt hydrate (Dich); $MgC1_2.6H_2O$, $CaCl_2$ and $CrCl_3.6H_2O$ were purchased from Sigma-Aldrich and used without further purification.

Synthesis of (Dich) coordination compounds: $[Mg(Dich)_2(H_2O)_4].5H_2O$, $[Ca(Dich)_2(H_2O)_4].2H_2O$ and $[Cr(Dich)_3(H_2O)_3].3H_2O$, were prepared by mixing appropriate salts ($MgC1_2.6H_2O$, $CaCl_2$ and $CrCl_3.6H_2O$) (1 mmol) dissolved in 20 ml of distilled water to Dich (2 mmol or 3 mmol), with molar ratio (1:2 or 1:3) dissolved in 20 ml of CH_3OH and refluxed for three hours. Then they were allowed to stand at room temperature for 2 days. The synthesized complexes were explained by FTIR, UV spectroscopy, C,H,N analyses, TG/DTG and magnetic susceptibility measurements.

$[Mg(Dich)_2(H_2O)_4].5H_2O$ complex (Dich/Mg): Dich solution of 0.581 g, 2 mmol in CH_3OH (20 ml) was mixed with an aqueous solution of $MgC1_2.6H_2O$ (0.204 g, 1 mmol) (20 ml). Then heat under reflux for 3 hours. A microcrystalline black precipitate was produced slowly by evaporation of the solvent and filtration. Dry under vacuum over anhydrous calcium chloride. Anal. Calc. for $C_{24}H_{30}Cl_4MgN_2O_{13}$: Carbon, 40.00%; Hydrogen, 4.20%; Nitrogen, 3.89%. Found: Carbon, 39.76%; Hydrogen, 4.08%; Nitrogen, 3.77%. Melting point > 250 ^oC and the yield is 75%.

$[Ca(Dich)_2(H_2O)_4].2H_2O$ complex (Dich/Ca): Dich solution of 0.581 g, 2 mmol in CH_3OH (20 ml) was mixed with an aqueous solution of $CaC1_2$ (0.111 g, 1 mmol) (20 ml). Heat under reflux for 3 hours. A microcrystalline black precipitate was produced slowly by evaporation of the solvent and filtration. Dry under vacuum over anhydrous calcium chloride. Anal. Calc. for $C_{24}H_{24}CaCl_4N_2O_{10}$: Carbon, 42.25%; Hydrogen, 3.55%; Nitrogen, 4.11%. Found: Carbon, 42.11%; Hydrogen, 3.40%; Nitrogen, 4.04%. Melting point > 250 ^oC and the yield is 79%.

$[Cr(Dich)_3(H_2O)_3].3H_2O$ complex (Dich/Cr): Dich solution of 0.871 g, 3 mmol in CH_3OH (20 ml) was mixed with aqueous solution of $CrC1_3.6H_2O$ (0.267 g, 1 mmol) (20 ml). Heat under reflux for 3 hours. A microcrystalline greenish black precipitate was produced slowly by evaporation of the solvent and filtration. Dry under vacuum over anhydrous calcium chloride. Anal. Calc. for $C_{36}H_{30}Cl_6CrN_3O_{12}$: Carbon, 44.98%; Hydrogen, 3.15%; Nitrogen, 4.37%. Found: Carbon, 44.80%; Hydrogen, 3.12%; Nitrogen, 4.19%. Melting point > 250 ^oC and the yield is 77%.

Type of analysis	**Models**
Elemental analyses	Perkin Elmer CHN 2400
Conductance	Jenway 4010 conductivity meter
FTIR spectra	Bruker FTIR Spectrophotometer
Electronic spectra	UV2 Unicam UV/Vis Spectrophotometer
Magnetic moment	Magnetic Susceptibility Balance
Thermo gravimetric	TG/DTG–50H, Shimadzu thermo-gravimetric analyzer
SEM	Quanta FEG 250 equipment
TEM	JEOL 100s microscopy

Animal model: Fifty (50) adult male Wistar rats were used in the current study. Animal experiments have been set following the approval of Taif University Animal Ethical Committee. The adult male albino rats were healthy, weighing 180–200 g. The animals were housed with food and water *ad libitum* under 12 hrs light/dark cycle to decrease the suffering. Male rats were divided into 5 groups. The healthy control non-treated groups were treated with a saline solution as a vehicle. There has also been no use of

analgesics or anti-inflammatory drugs. 2nd group was treated with AC in a dose of 500 mg/Kg[12]. The other three groups Ca/Dich, Mg/Dich and Cr/Dich were injected as previously described to the dose of dichlorobenzene (3.6 mmol/kg)[13]. The experiment period was carried for 30 successive days.

Experimental Design: The experimental animals were divided into 5 groups as follows: 1st control group was given saline solution (1 ml/kg) ; 2nd Group was given AC at a dose of 500 mg/kg[12]; 3rd , 4th and 5th groups were treated with Ca/Dich , Mg/Dich and Cr/Dich successively in a dose of (3.6 mmol/kg)[13].

Tissue homogenates preparation for measurement of oxidative stress markers: Renal tissue portions (~ 0.25 g) were used for determination of the oxidative stress markers. Renal tissues were perfused with buffer phosphate saline (pH=7.4) and then we added a protease inhibitor to protect the renal antioxidant enzymes which are very sensitive to the oxidation.

Oxidative and antioxidant biomarkers activity: MDA levels were evaluated according to Ohkawa et al[14]. Superoxide dismutase (SOD) activity was evaluated by Marklund and Marklund[15]. Catalase (CAT) was estimated by Aebi[16]. Glutathione (GSH) was assessed by Couri and Abdel-Rahman[17]. Glutathione peroxidase (GPx) was estimated by Hafeman et al[18]. Myeloperoxidase (MPO) was estimated according to Suzuki et al[19]. Xanthine oxidase (XO) was evaluated by Litwack et al[20].Total thiol level was estimated according to Hu[21].

IL-6 and TNF-α activities in the liver homogenates: Cytokine levels of (IL-6 and TNF-α) were evaluated by using (ELISA) kit of " Immuno-Biological Laboratories", USA.

Lipid profile: Total cholesterol (TC) and triglycerides (TG) were estimated according to Carr et al.[22] (HDL–c) was estimated according to Warnick et al[23]. (LDL–c) level was evaluated according to Friedewald[24]. The protein level was measured according to Bradford[25].

Liver function biomarkers: Serum AST and ALT enzymes were evaluated according to Reitman and Frankel[26]. ALP was measured according to Young et al[27] by using commercial kit "Biodiagnostic kits". LDH was determined according to Vassault[28] by using "BioVision Colorimetric Assay Kit " Milpitas, CA 95035 USA.

Kidney function biomarkers: Creatinine and uric acid were estimated according to Schirmeister et al[29] and Fossati et al.[30] The urea level was estimated according to Patton and Crouch[31].

Inflammation marker (CRP) activity: CRP levels were evaluated according to Wener et al[32] by using SEA821 (ELISA) Kit.

Mitochondrial function

Evaluation of succinate dehydrogenase (SDH, complex II) activity: Metabolic viability based assay is used for measuring the mitochondrial metabolic rate and reflects indirectly the number of the viable cells. The mitochondrial SDH activity was evaluated also. The absorbance was measured using an ELISA kit at 570 nm (Tecan, Rainbow Thermo, Austria)[33].

Mitochondrial ROS assay: The mitochondrial ROS generation was evaluated using the dichlorodihydrofluorescein diacetate (DCFH-DA) probe. An increase in fluorescence intensity indicates an increase in ROS generation due to exposure to inflammation of hepatotoxicity[33].

Mitochondria membrane potential (MMP, ΔΨm) assay: The mitochondria of the hepatic tissues were isolated from all groups. Briefly, the mitochondrial ROS generation was evaluated using rhodamine 123 (Rh123) probe at a final concentration of 10 μM for 30 min at 30 °C. An increase in fluorescence intensity indicates an increase in the collapse of MMP[34].

Fluorescent detection of mitochondrial membrane potential: Animals were sacrificed, hepatic tissues were washed thoroughly and rinsed with ice. They were gently blotted between the folds of a filter paper and weighed in an analytical balance. 10% of homogenate was prepared in 0.05 M phosphate buffer (pH 7) using a polytron homogenizer at 40°C according to manual instructions. Fluorescent kit cannot be measured and then using Fluorometer microplate reader (Thermo Fisher Scientific Oy FI-01621 Vantaa, Finland), Mitochondrial membrane potential was expressed as JC-1 fluorescence ratio (J-aggregates: J-monomers).

Evaluation of swelling on mitochondria: Briefly, swelling of mitochondria in sizes of 10 and 100 nm (pure and impure) was measured using an ELISA reader (Tecan, Rainbow Thermo) at 540 nm. A decrement in absorbance indicates an increment in mitochondria swelling[35].

Cytochrome c oxidase release assay: Evaluation of cytochrome c release that referred to mitochondrial volume was measured (Rat/Mouse cytochrome c Immunoassay kit, USA).

ATP content assay: The ATP content was detected using the luciferase enzyme. The intensity was evaluated using Sirius tube luminometer (Berthold Detection System, Germany). ATP content was expressed as nmol/mg protein[36].

Histological examination and transmission electron microscopy (TEM) evaluation: Liver and kidney portions were fixed in about "10% neutral buffer formalin" and then other processing was carried out as described previously by Gabe[37]. For ultrastructural examination, the hepatic and

renal tissues were fixed in 2.5% glutaraldehyde for about 48 h and then the other TEM processing according to Weakley et al[38].

Single cell gel electrophoresis (SCGE) (Comet assay): Renal tissues were placed in a small Petri dish with a solution ice-cold ($Ca^{2+}$and Mg^{2+},20 mM EDTA and 10% DMSO). The cells viability was examined by using the comet images after the electrophoresis et al[39]. The comet assay was described previously as by Collins and Dunsinka[40].

RNA isolation and RT-PCR analysis: Total RNA was isolated from the hepatic cells by using trizol reagent (Invitrogen). RNA was preserved at -80 ºC. RNA (1 µg) was used for reverse transcription reaction using reverse transcriptase, reverse primer, deoxyribonucleotide triphosphate and 1U RNase inhibitor. The reaction was incubated at 42ºC for 1 h. The PCR reactions were carried out in a total volume of 20 µl containing *Taq* DNA polymerases, 0 dNTP, reaction buffer and forward and reverse primers as follows:

	Forward	**Reverse**
TNF-α	5′-AGC-ACA-GAA-AGC-ATGATC-CG-3′	5′-GTT-TGC-TAC-GAC-GTG-GGC-TA-3
IL-6	5′-CGA-TGA-TGC-ACT-TGC-AGA-AA-3′	5′-TGG-AAA-TTG-GGG-TAGGAA-GG-3′

After the initial denaturation at 95 ºC, the amplification by 35 cycles of 93 ºC for 40 seconds (denaturing), 50-52 ºC for 40 sec (annealing), 73 ºC for 40 sec (extension) occurred. The PCR products were analyzed by 1.5% agarose gel electrophoresis. The mRNA expression level was quantitated by Bio-Rad Quantity One software.

Statistical analysis: Data are expressed as "mean ± SE". Statistical analysis was performed by using two-way Analysis of Variance (ANOVA). The statistical significance was set at $P < 0.05$. All statistical analyses were performed using SPSS statistical version 20 software package (SPSS Inc., USA). We used post hoc test to detect the significance ratio.

Results

Structure interpretations of Mg^{II}, Ca^{II} and Cr^{III} Dich complexes

Conductance measurements: Mg(II), Ca(II) and Cr(III)–Dich complexes are insoluble in methanol, ethanol, acetone, $CHCl_3$ and water while there are soluble in DMSO and DMF. The molecular structure formula of the synthesized complexes (Fig. 1) was speculated depend on elemental analysis and infrared assignments. The experimental data of these complexes is in agreement with the calculated data. At room temperature, the conductivity values of the Dich complexes which were dissolved in Dimethyl sulfoxide solvent with 10^{-3} M concentration are matched with the non-electrolytic behavior (7.0-12 $ohm^{-1}.cm^2.mol^{-1}$)[41]. The purity of the synthesized Dich complexes was checked by C,H,N analysis, FTIR, SEM.

Infrared spectroscopy: The infrared frequencies (cm^{-1}) of both Dich chelate and its Mg(II), Ca(II) and trivalent Cr complexes are presented in table 1. The infrared spectrum of the Dich free ligand (Fig. 2a) and the spectra of the synthesized complexes (Fig. 2b) were assigned in order to be recognized to the place of coordination between Dich ligand and the respected metal ion after complexation. Infrared spectrum of the Dich free ligand has some characteristic bands present at 3376 and 3144 cm,$^{-1}$ 2954, 2762 and 2735 cm^{-1}, 1631 cm^{-1}, 1589 cm^{-1}, 1564–1428 cm^{-1}, 1311, 1174 cm^{-1}, 1256 cm^{-1} and 867–614 cm^{-1} assigned to ν(O–H) hydrated water molecules, ν(C–H) two aromatic rings (2,6-dichloro-4-imino-cyclohexa-2,5-dienone and phenolic), ν(C=O) of 2,6-dichloro-4-imino-cyclohexa-2,5-dienone ring, ν(C=N, 2,6-dichloro-4-imino-cyclohexa-2,5-dienone ring), ν(C=C) aromatic, ν_{as}(C–N–C), ν_s(C–N–C) ν(C–O) and ν(C–Cl) halo organic compound, respectively[41].

Magnesium, calcium and chromium complexes have distinguish bands at 3201-2030 cm^{-1} and 790-761 cm^{-1} regions due to the vibrations motions of coordinated water molecules[42,43]. The stretching vibration band at 1631 cm^{-1} is attributed to the carbonyl group of the 2,6-dichloro-4-imino-cyclohexa-2,5-dienone ring, this band is shifted to higher frequencies (1712–1699 cm^{-1}) after coordination, this refers to that the Dich ligand is not coordinated to metal ions through the oxygen of carbonyl group. The stretching vibration bands of phenolic C–O appeared at 1256 cm^{-1} in the Dich chelat[44] and shifted towards lower frequencies by ~ 22-28 cm^{-1} in the complexes (Table 1).

This shift confirms the coordination of oxygen of phenolic group towards metal ions with formation of the C–O–M bond. The medium intensities bands observed in case of the synthesized complexes within the region 540–500 cm^{-1} and were assigned to ν(M–O)[44]. In case of Mg(II), Ca(II) and Cr(III) complexes, the stretching frequencies of C=N and C=C bands shifted from 1564–1428 cm^{-1} to 1565–1400 cm^{-1},[44-46] these shifts may be attributed to conjugation as well as changes in electron density through the aromatic rings. Therefore, it can be deduced that the Dich ligand acts as monodentate chelate and is coordinated to the metal ion through oxygen of phenolic ring moiety (Fig. 1).

Electronic and magnetic measurements: The assignment of various d-d transitions and charge transfer bands in the spectrum of the chromium(III) complex are based on the works of Lever[47] and Cotton Wilkinson et al[48]. The electronic spectrum of chromium(III) complex was scanned in DMSO at room temperature. The electronic spectrum of Cr(III) complex exhibited three bands at 520 nm (ν_1), 434 nm (ν_2) and 375 cm^{-1} (ν_3) corresponding to $^4A_{2g} \rightarrow {}^4T_{2g}(F)$ and $^4A_{2g} \rightarrow {}^4T_{1g}$ (F) and $^4A_{2g} \rightarrow {}^4T_{1g}(P)$ transitions respectively characteristics of octahedral geometry around

the Cr(III) ion[47]. The magnetic moment value obtained for Cr(III) complex lies at 3.91 BM that corresponds to octahedral field.

The Dich is black blue in color and this color has a maximum wavelength at λ_{max} 629 nm. This band obviously existed in the the complexes with shifting to higher wavelength at about ~640 nm under complexation. The magnetic susceptibilities data of Mg(II) and Ca(II) coordination compounds have a diamagnetic nature as expected for a d^{10} system, i.e. paired electron in valence shell orbital or invisibility of unpaired electron.

Thermal analysis: The thermal decomposition curves (TG-DrTGA) of Mg(II), Ca(II) and Cr(III) complexes display a mass loss within temperature range 30–250 °C indicating that uncoordinated and coordinated water molecules are present in the complexes (Fig. 3a-c). The complexes do not show any mass loss up to 800 °C, this reveals that thermal stability. The TG curves in the 200–800 °C range with DTG_{max} at 275 °C, 240 and 450 °C and 240, 275 and 320 °C in case of Mg(II), Ca(II) and Cr(III) respectively and suggest that the mass loss for all three complexes corresponds to decomposition of Dich ligands.

In all cases the remaining residues are metal oxides (MgO, CaO and ½Cr_2O_3). These results are in agreement with the composition of the complexes, mass loss (Calc.) Found. for $[Mg(Dich)_2(H_2O)_4].5H_2O$, $[Ca(Dich)_2(H_2O)_4].2H_2O$ and $[Cr(Dich)_3(H_2O)_3].3H_2O$ are (94.41) 93.85%, (91.78) 91.50% and (92.09) 91.65% respectively.

Table 1
Infrared spectral data (cm^{-1}) of Dich complexes

Compounds	Frequencies, cm^{-1}				
	ν(O–H)	ν(C=O)	ν(C-O)	ν(C-Cl)	ν(M-O)
Dich	3376-3144	1631	1256	867-614	429
Mg(II)	3201, 3049	1699	1228	1001-623	535
Ca(II)	3195, 3043	1700	1226	1096-640	531
Cr(III)	3200, 3030	1712	1234	1004-620	540, 500

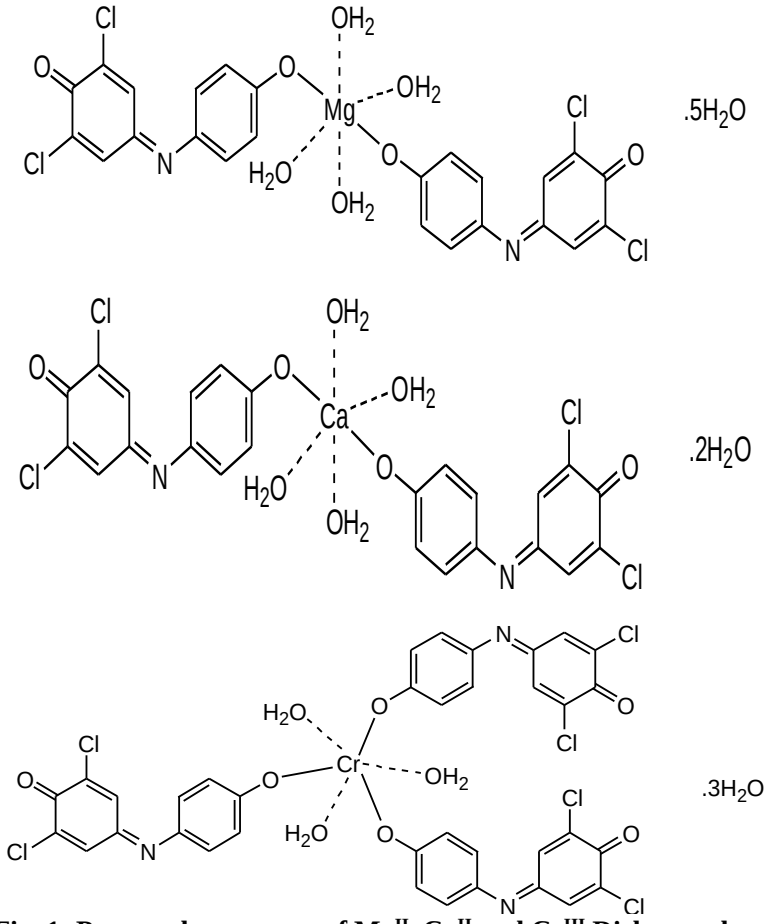

Fig. 1: Proposed structures of Mg^{II}, Ca^{II} and Cr^{III} Dich complexes

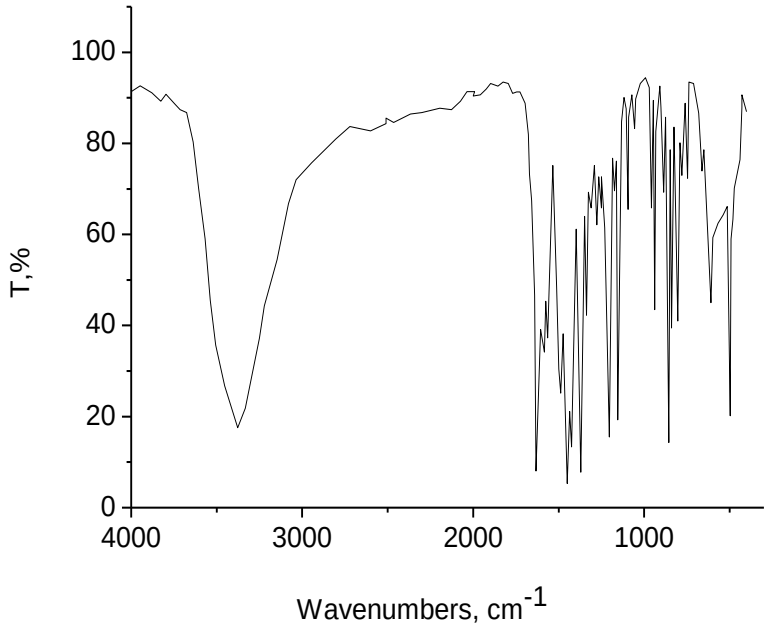

Fig. 2a: Infrared spectrum of Dich free ligand

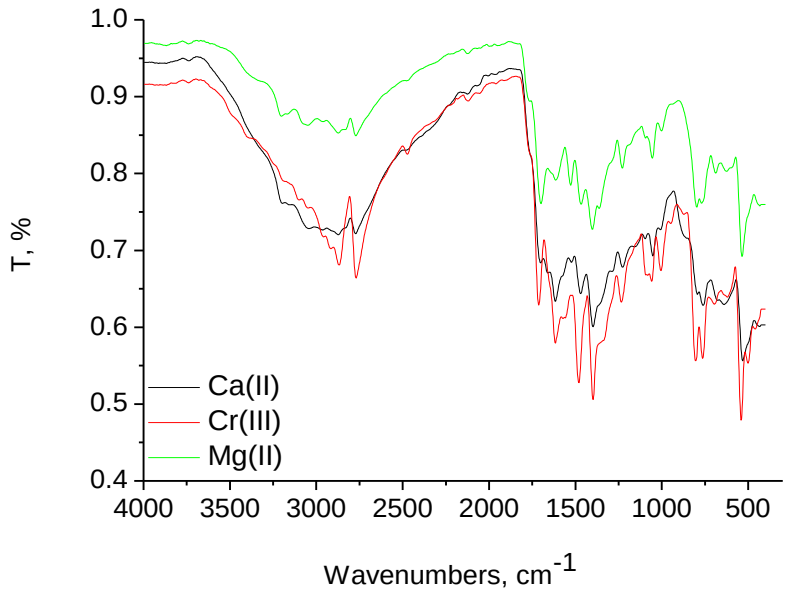

Fig. 2b: Infrared spectrum of Mg^{II}, Ca^{II} and Cr^{III} Dich complexes

SEM and TEM morphological investigations: The surface morphology and the size particles regarding Mg(II), Ca(II) and Cr(III) Dich complexes have been investigated using scanning (SEM) and transmission (TEM) electron microscopes. Fig. 4a–c and fig. 5a–c refer to the SEM and TEM photographs of the synthesized Mg(II), Ca(II) and Cr(III) complexes. It was proved that there is a uniform matrix of the synthesized complexes in the images. This can be deduced that the synthesized complexes have a homogeneous phase material. A compressed slice like shape is observed in the Mg(II) complex (Fig. 4a) with the particle size of 5µm. A single phase formation of Ca(II) complex having spherical stones morphologies with particle size 5 µm is displayed in fig. 4b.

The image of Cr(III) complex (Fig. 4c) shows sheets like shape with 5 µm particle size. Figure 5a–c shows the TEM images of the prepared Dich nanoparticles complexes, these indicate that Mg(II), Ca(II) and Cr(III) nanoparticle complexes are approximately spherical black spots shape with the diameter 54-91 nm, 85-135 nm and 42-77 nm respectively.

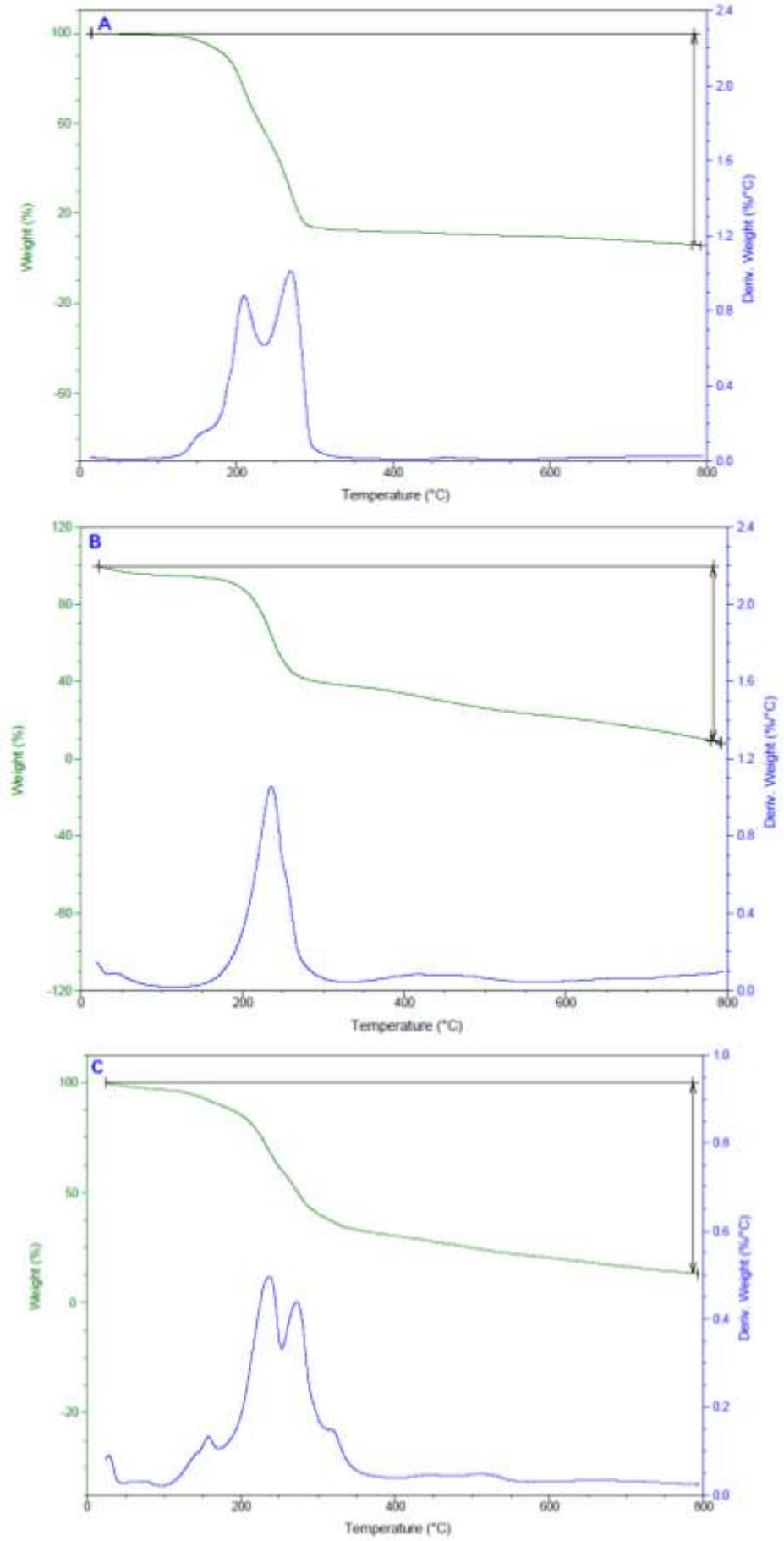

Fig. 3: TG-DTG curves of A: Mg^{II}, B: Ca^{II} and C: Cr^{III} Dich complexes

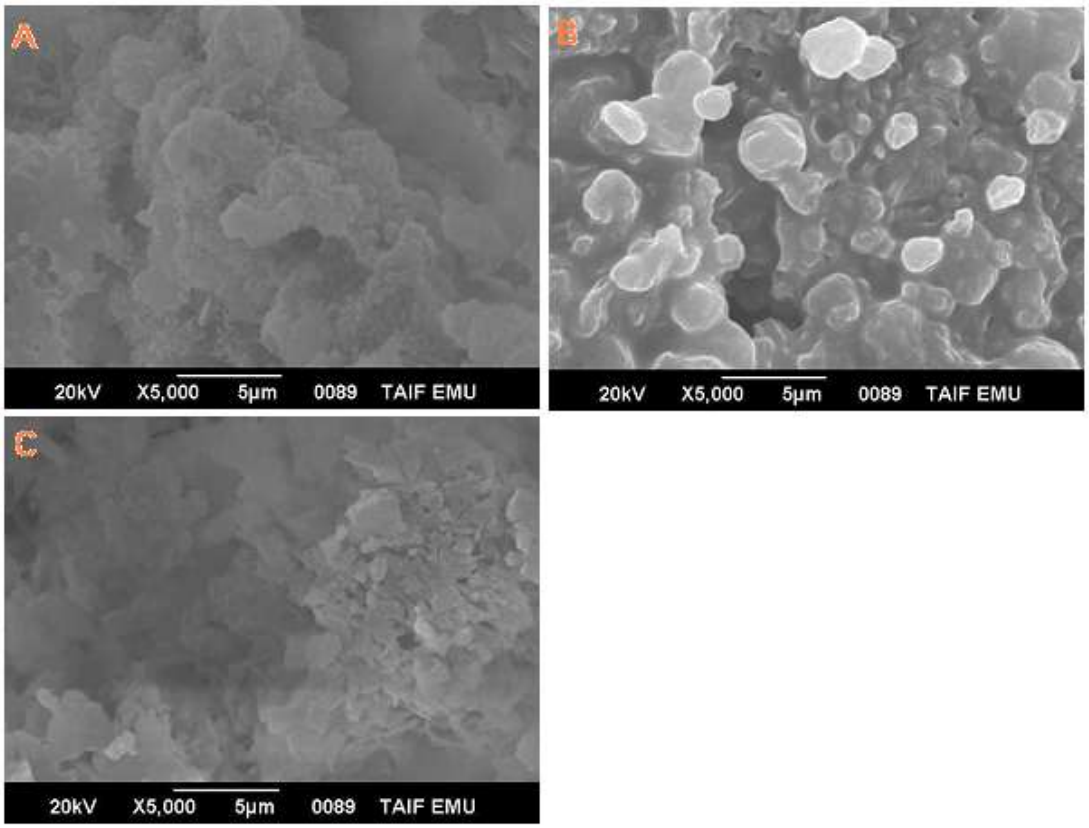

Fig. 4: SEM images of A: Mg^{II}, B: Ca^{II} and C: Cr^{III} Dich complexes

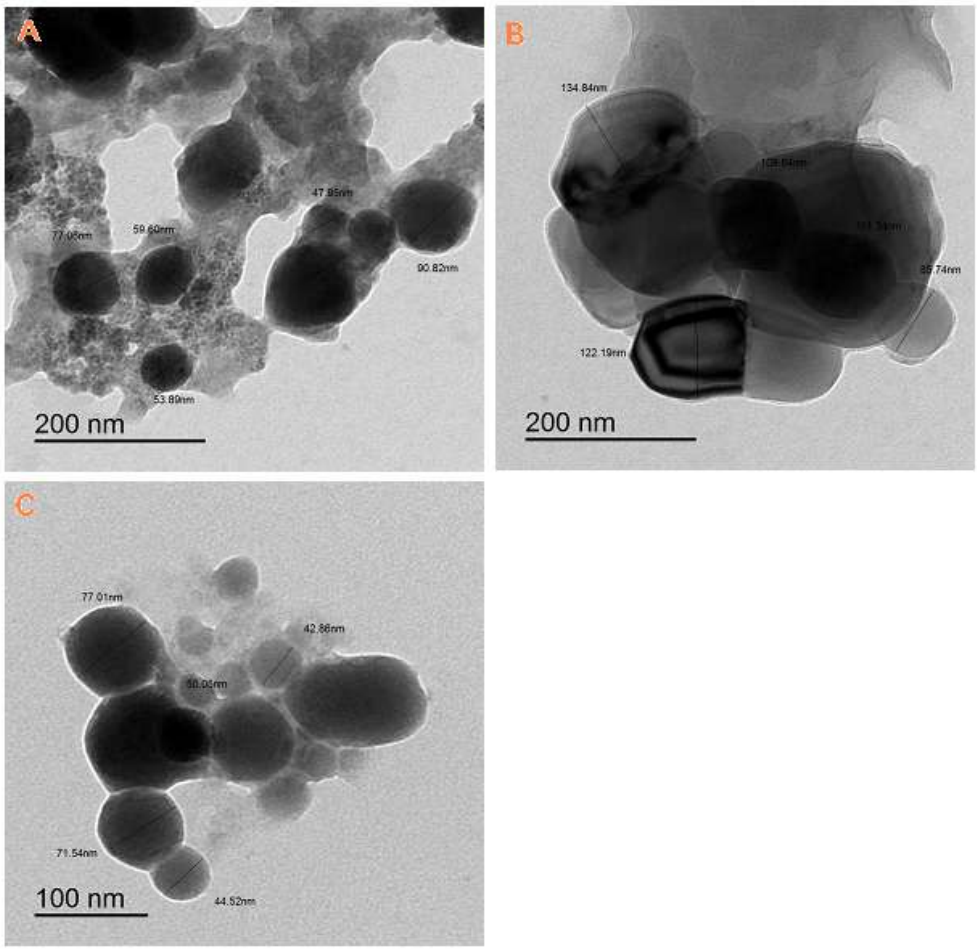

Fig. 5: TEM images of A: Mg^{II}, B: Ca^{II} and C: Cr^{III} Dich complexes

Hepatic biomarkers and lipid profile: The ALT, AST, ALP and LDH activities were significantly elevated in AC group (Table 2) while these levels significantly declined in the groups treated with either Ca/ Dich, Mg/ Dich and Cr/ Dich and restored to about control levels except total proteins which were declined in AC group and elevated in other treated groups with AC and accompanied with Ca/ Dich, Mg/Dich and Cr/Dich.

Treatment of the rats with AC caused a significant increment in TG, TC, LDL-c and vLDL-c with declining HDL-c level as compared to control group (Table 3). While these levels were equal to the levels of control group in Ca/ Dich, Mg/Dich and Cr/Dich treated groups, these novel complexes succeeded in improving the lipid profile picture acting as hypocholestermic agents.

Renal biomarkers: Urea, uric acid and creatinine levels were significantly elevated in AC group (Table 4), while these levels were significantly declined in the groups treated with either Ca/ Dich, Mg/ Dich and Cr/ Dich and restored to about control levels.

Table 2
Changes in hepatic enzymes and biomarkers in male rats treated with Acrylamide (AC) Ca/Dich, Mg/Dich and Cr/Dich on male rats.

Parameters / Groups	Control	AC	AC+ Ca/ Dich	AC+ Mg/ Dich	AC+ Cr/ Dich
ALT (U/L)	12.41 ± 1.16^{b}	178.45 ± 6.62^{a}	12.25 ± 0.32^{b}	12.38 ± 1.19^{b}	12.36 ± 1.44^{b}
AST (U/L)	13.15 ± 0.35^{b}	293.55 ± 7.36^{a}	13.15 ± 1.22^{b}	13.26 ± 1.49^{b}	13.14 ± 1.29^{b}
ALP (U/L)	22.40 ± 1.45^{b}	198.46 ± 5.23^{a}	22.35 ± 1.02^{b}	21.29 ± 8.69^{b}	22.98 ± 5.78^{b}
LDH (U/L)	100.83 ± 7.02^{b}	585.95 ± 9.31^{a}	101.15 ± 1.25^{b}	100.49 ± 4.85^{b}	100.29 ± 5.49^{b}
Total proteins (g/dL)	8.50 ± 0.86^{bc}	3.10 ± 1.06^{a}	8.12 ± 0.49^{c}	8.72 ± 2.16^{bc}	8.59 ± 1.36^{bc}

ALT: Alanine aminotransferase; AST: Aspartate aminotransferase; ALP: Alkaline phosphatase; LDH: lactate dehydrogenase; AC, Acrylamide; Ca/Dich, Ca/2,6-Dichloroindophenol; Mg/ Dich, Mg/2,6-Dichloroindophenol; and Cr/ Dich, Cr/2,6-Dichloroindophenol. Values are expressed as means ± SE; n =10 for each treatment group. symbols are arranged alphabetically indicate significance comparison as compared to control group and other treated groups from higher to lower ($p< 0.05$).

Table 3
Changes in lipid profile in male rats treated with Acrylamide (AC), Ca/Dich, Mg/Dich and Cr/Dich on male rats.

Parameters / Groups	Control	AC	AC+ Ca/ Dich	AC+ Mg/ Dich	AC+ Cr/ Dich
TG (mg/dl)	70.15 ± 5.36^{bc}	199.48 ± 8.22^{a}	68.36 ± 2.36^{c}	70.32 ± 5.25^{bc}	68.02 ± 4.25^{c}
TC (mg/dl)	140.25 ± 6.03^{bc}	385.49 ± 7.65^{a}	139.56 ± 5.46^{c}	138.36 ± 4.45^{c}	139.36 ± 3.85^{c}
HDL-c	42.95 ± 4.36^{a}	20.03 ± 3.78^{b}	42.03 ± 2.65^{a}	42.65 ± 3.65^{a}	42.32 ± 4.36^{a}
LDL-c	30.06 ± 2.56^{b}	49.38 ± 4.16^{a}	30.02 ± 2.65^{b}	30.07 ± 1.64^{b}	30.02 ± 2.82^{b}
vLDL-c	13.80 ± 1.03^{b}	30.13 ± 2.06^{a}	13.27 ± 1.25^{b}	13.46 ± 1.35^{b}	13.40 ± 1.26^{b}

HDL-c; High density lipoprotein, LDL-c: Low density lipoprotein; vLDL-c: very low density lipoprotein; AC, Acrylamide; Ca/ Dich, Ca/2,6-Dichloroindophenol; Mg/ Dich, Mg/2,6-Dichloroindophenol and Cr/ Dich, Cr/2,6-Dichloroindophenol.
Values are expressed as means ±SE; n = 10 for each treatment group.
symbols are arranged alphabetically indicate significance comparison as compared to control group and other treated groups from higher to lower ($p< 0.05$).

Table 4
Changes in kidney functions in male rats treated with Acrylamide (AC), Ca/Dich, Mg/Dich and Cr/Dich on male rats.

Parameters / Groups	Control	AC	AC+ Ca/ Dich	AC+ Mg/ Dich	AC+ Cr/ Dich
Urea (gdl^{-1})	20.03 ± 1.03^{c}	39.25 ± 2.68^{a}	20.92 ± 0.87^{bc}	20.48 ± 2.02^{c}	21.37 ± 1.68^{c}
Uric acid (gdl^{-1})	14.09 ± 1.14^{c}	29.87 ± 2.68^{a}	14.59 ± 1.58^{c}	14.98 ± 2.14^{bc}	14.24 ± 1.69^{c}
Creatinine (gdl^{-1})	0.54 ± 0.01^{b}	2.98 ± 0.58^{a}	0.56 ± 0.07^{b}	0.55 ± 0.09^{b}	0.57 ± 0.04^{b}

HDL-c; High density lipoprotein, LDL-c: Low density lipoprotein; vLDL-c: very low density lipoprotein; AC, Acrylamide; Ca/ Dich, Ca/2,6-Dichloroindophenol; Mg/ Dich, Mg/2,6-Dichloroindophenol; and Cr/ Dich, Cr/2,6-Dichloroindophenol.
Values are expressed as means ±SE; n = 10 for each treatment group.
symbols are arranged alphabetically indicate significance comparison as compared to control group and other treated groups from higher to lower ($p< 0.05$).

Tumor necrosis marker, interleukin-6 and CRP level: There were no changes in the levels of TNF-α and IL-6 in the rats that were treated with Ca/ Dich, Mg/Dich and Cr/Dich as compared to the control group (Table 5). The elevation of the inflammatory cytokines was observed in the AC group. The anti-inflammatory effect was noticed in the combined group treated with AC in combination with Ca/ Dich, Mg/ Dich and Cr/ Dich respectively.

The CRP levels were increased in AC group as compared to control group. The decrease of CRP in AC plus Ca/ Dich, Mg/ Dich and Cr/ Dich was compared to its related group of AC alone.

Oxidative stress biomarkers: The SOD activity was significantly declined in AC treated group (Table 6). CAT and GPx activities were also declined in AC treated group and did not change in other treated groups with Ca/ Dich, Mg/ Dich and Cr/ Dich.

GPx levels were significantly declined in AC treated group as compared to control group (Table 6) while GPx was in normal level as control group in groups treated with AC in combination with Ca/ Dich, Mg/ Dich and Cr/ Dich respectively.

There was a significant elevation in MDA activity in the rats treated with AC. No critical changes were recorded in MPO levels of all treated groups except the AC treated animals (Table 7). MPO activities were increased in AC treated group as compared to control group as well as in AC combined with Ca/ Dich, Mg/ Dich and Cr/ Dich as compared to its relative group of AC respectively (Table 7).

In AC group, thiol activity was declined as compared to the control group (Table 7). In Ca/ Dich, Mg/ Dich and Cr/ Dich combined with AC group, the thiol activity declined respectively as compared to the control group. MPO level was significantly elevated in AC treated group while it declined in the other groups treated with AC in combination with Ca/ Dich, Mg/ Dich and Cr/ Dich (Table 7).

SDH, ROS and MMP: The ROS increased significantly in DG group by 3.5-fold as compared to control group (Fig. 4). Treatment the animals with CNPs in two doses (LD and HD) or V or both of them lowered the ROS by 50.7%, 56.9% and 74.8% as compared to DG-treated rats respectively.

Table 5
Changes in serum TNF-α , Il-6 and CRP level in male rats treated with Acrylamide (AC) , Ca/Dich , Mg/Dich and Cr/Dich on male rats.

Parameters / Groups	Interleukin-6 (IL-6) (Pg/g) tissue	Tumor necrosis factor Alpha (TNF-α) (Pg/g) tissue	CRP (mg/L)
Control	3.16±1.02^{c}	5.58±0.78^{bc}	4.23±0.22^{bc}
AC	20.16±3.02^{a}	30.03±3.03^{a}	24.34±2.23^{a}
AC+ Ca/ Dich	3.59±0.17^{bc}	5.05±0.59^{c}	4.11±1.45^{c}
AC+ Mg/ Dich	3.52±0.87^{c}	5.19±0.95^{c}	4.13±1.59^{c}
AC+ Cr/ Dich	3.43±0.29^{c}	5.15±0.52^{c}	4.16±1.46^{c}

TNF-α: Tumour necrosis factor Alpha; IL-6: Interleukin-6; AC, Acrylamide; Ca/ Dich, Ca/2,6-Dichloroindophenol; Mg/ Dich, Mg/2,6-Dichloroindophenol; and Cr/ Dich, Cr/2,6-Dichloroindophenol.
Values are expressed as means ±SE; n = 10 for each treatment group.
symbols are arranged alphabetically indicate significance comparison as compared to control group and other treated groups from higher to lower.

Table 6
Effect of with Acrylamide (AC), Ca/Dich, Mg/ Dich and Cr/Dich on male rats on antioxidant markers in kidney homogenates in male rats.

Parameters / Groups	Catalase (CAT) (U/g)	Glutathione peroxidase (GPx) (U/g)	Malondialdehyde (MDA) (U/g)	Super oxide dismutase (SOD) (U/g)
Control	8.09±1.13^{a}	13.13±2.16^{b}	5.39±1.05^{c}	20.13±1.17^{b}
AC	1.36±0.15^{b}	6.52±2.41^{c}	51.52±3.22^{a}	9.52±1.25^{c}
AC+Ca/ Dich	8.15±1.03^{a}	13.48±0.85^{ab}	5.92±0.35^{bc}	21.85±1.05^{ab}
AC+Mg/ Dich	8.25±1.36^{a}	13.25±1.47^{b}	5.81±0.24^{c}	20.74±1.07^{b}
AC+Cr/ Dich	8.23±1.54^{a}	13.47±0.36^{ab}	5.92±0.12^{bc}	21.03±1.23^{ab}

SOD: superoxide dismutase; MDA: malondialdehyde; GPx: Glutathione peroxidase; CAT: catalase, AC, Acrylamide; Ca/ Dich, Ca/2,6-Dichloroindophenol; Mg/ Dich, Mg/2,6-Dichloroindophenol; and Cr/ Dich, Cr/2,6-Dichloroindophenol.
Values are expressed as means ± SE; n = 10 for each treatment group, symbols are arranged alphabetically indicate significance comparison as compared to control group and other treated groups from higher to lower ($p< 0.05$)

The cell viable number was detected by SDH% as presented in fig. 4. The SDH was 93.4% in control group and decreased significantly to 54% in DG-treated rats while the groups treated with DG combined with CNPs (LD and/or HD) and V elevated the percent of SDH to about 82 and 87% respectively.

The baseline value of ROS for normal healthy rats was 18 ± 1.5 as shown in fig. 4. The aging rats presented higher ROS content than controls for mitochondria (5.4-fold). The ROS generation decreased by 67.1% in CNPs (LD and HD). More reduction in ROS contents was observed in V, CNPs (LD) and CNPs (HD) in combination with DG 71.6% and 73.4% respectively.

On day 60, the effects of chitosan or/and vanillin on MMP ($\Delta\psi m$) were illustrated in fig. 6. The DG group significantly increased MMP compared with the control of healthy rats, which was notably to be decreased by the combination of CNPs (LD and HD) and V in this sequence. These results suggested that CNPs and V in combination was a remarkably enhanced collapse of MMP in DG rats.

Aging accelerated mitochondrial swelling was illustrated in fig. 6 where it was elevated as compared to control healthy rats. The swelling diminished for either CNPs either LD or HD either alone or in combination with V respectively.

Aging rats release less ATP content as compared to the control rats (Fig. 7). CNPs (LD and HD) treatment increased the ATP content as compared to DG animals. Similarly, CNPs (LD and HD) with V in combination with DG treatment elevated ATP content separately. So, there was a synergistic effect between CNPs in two doses especially CNPs(HD) and V and acting as energy promoters and oxidative injury inhibitors.

Table 7
Changes in serum hepatic Myloperoxidase antioxidant enzymes and thiol level in male rats treated with Acrylamide (AC), Ca/Dich , Mg/Dich and Cr/Dich on male rats.

Parameters / Groups	myeloperoxidase (MPO) (nmol/min/mL)	Hepatic thiol (µmol/g)
Control	13.16±1.85^{b}	7.20±1.16^{b}
AC	39.66±1.62^{a}	3.01±0.53^{c}
AC+ Ca/ Dich	13.04±1.56^{b}	7.54±0.76^{ab}
AC+ Mg/ Dich	13.06±1.66^{b}	7.39±0.73^{b}
AC+ Cr/ Dich	13.36±1.80^{b}	7.32±0.36^{b}

MPO: myeloperoxidase; XO: Xanthine oxidase, AC, Acrylamide; Ca/ Dich, Ca/2,6-Dichloroindophenol; Mg/ Dich, Mg/2,6-Dichloroindophenol; and Cr/ Dich, Cr/2,6-Dichloroindophenol.Values are expressed as means ±SE; n = 10 for each treatment group. symbols are arranged alphabetically indicate significance comparison as compared to control group and other treated groups from higher to lower ($p< 0.05$).

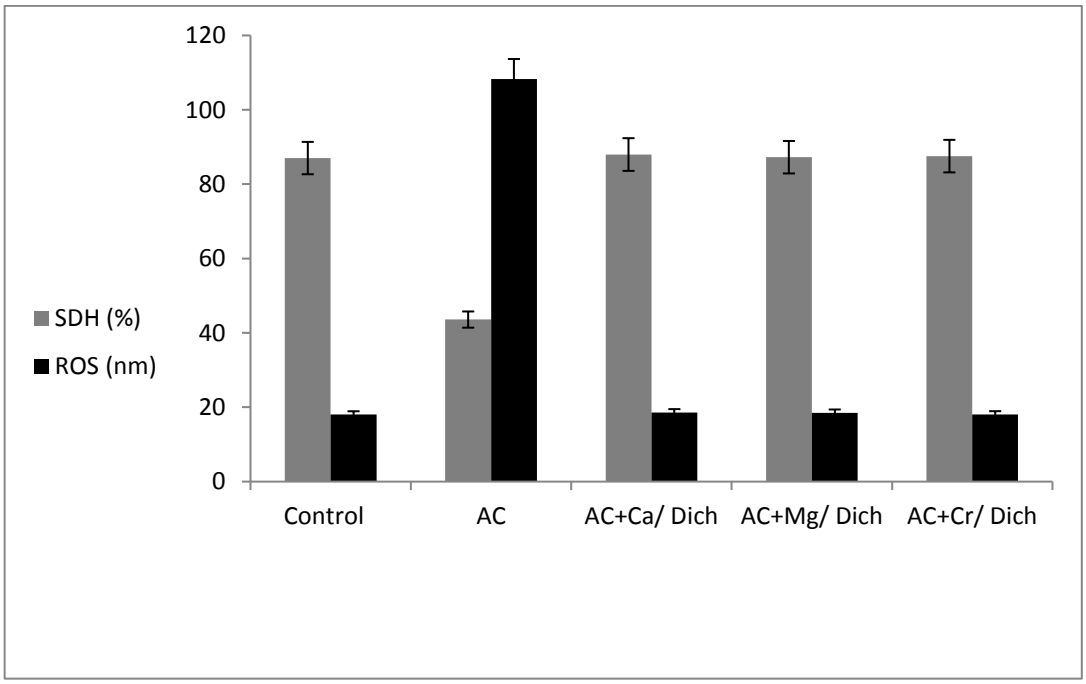

Fig. 6: The efficacy of Ca/Dich, Mg/Dich and Cr/Dich against succinate dehydrogenase (SDH) and reactive oxygen species (ROS) in the rat model of nephrotoxicity and hepatotoxicity induced by Acrylamide (AC)

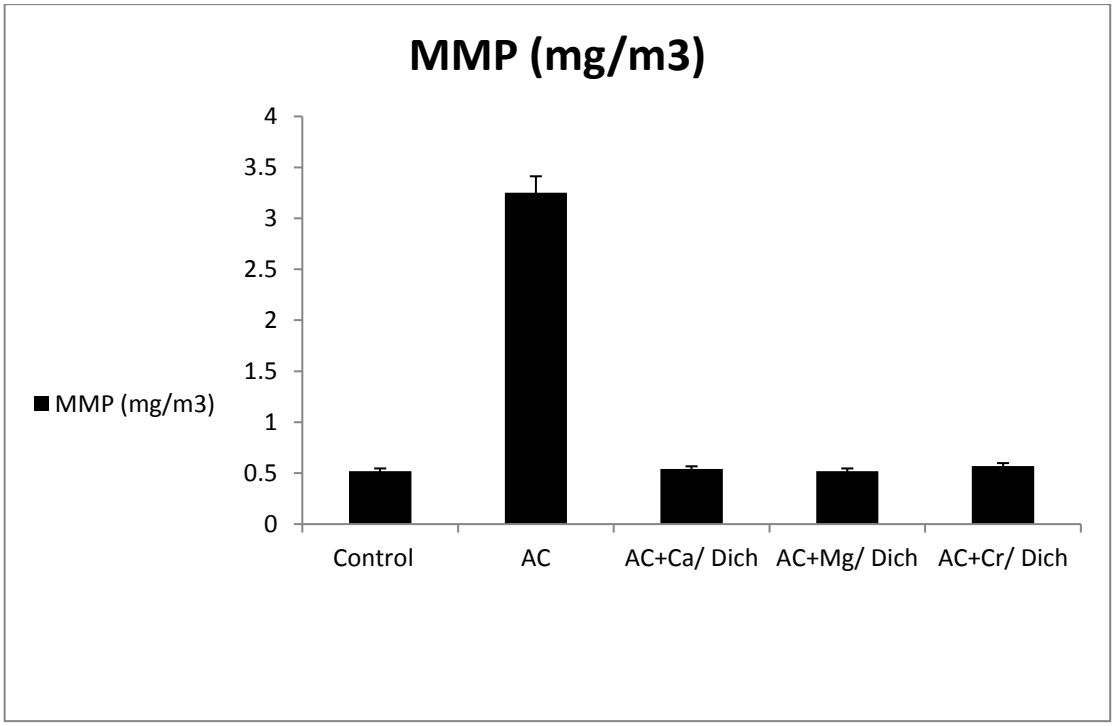

Fig. 7: The efficacy of Ca/Dich, Mg/Dich and Cr/Dich against mitochondrial membrane potential (MMP) in the rat model of nephrotoxicity and hepatotoxicity induced by Acrylamide (AC)

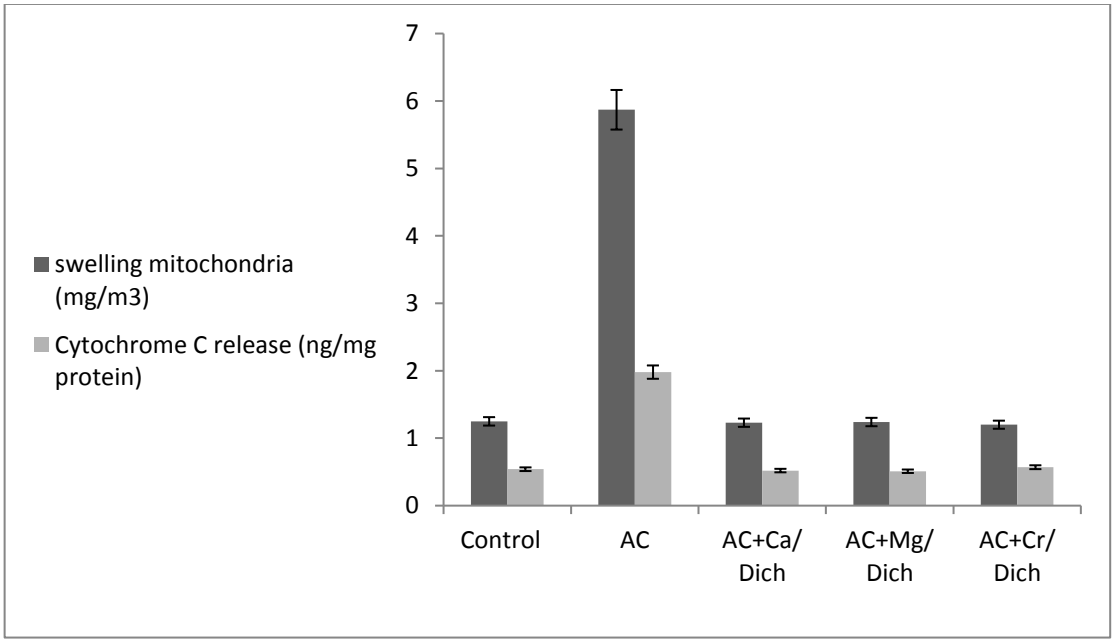

Fig. 8: The efficacy of Ca/Dich, Mg/Dich and Cr/Dich against swelling mitochondria (mg/m3) and cytochrome C release (ng/mg protein) in the rat model of nephrotoxicity and hepatotoxicity induced by Acrylamide (AC)

Transmission electron microscope (TEM) evaluation: Electron micrograph of liver sections (Fig. 10) (A) Control group showed the normal hepatocytes with normal nuclei and normal sized mitochondria and normal endoplasmic reticulum with appearance of normal glycogen granules, (B) AC treated group showed pyknotic nuclei with irregular nuclear boundaries and disintegration of most hepatic structures with severe fatty change and appearance of large vacuoles. C, D and E AC treated groups with either Ca/Dich, Mg/Dich and/or Cr/Dich had normal appearance of hepatic structures with normal rounded nucleus, regular nuclear bounderies, normal mitochondria and normal endoplasmic reticulum with normal sized vacuoles in the cytoplasm.

Electron micrograph of kidney section: (A) Control group showed normal homogenous chromatin nucleus, vacuoles, filtration membrane, nucleus of podocyte with expansion of mesangial substance, basal lamina, capillary lumen and red blood cells. (B) Group treated with AC treated group showed detached pedicles, disintegration of most of renal tissues,

appearance of enlarged capillary lumen with enlarged Bowman's space, appearance of pyknotic nuclei with disintegrated chromatin, presence of excessive red blood cells, appearance of thick basal lamina with appearance of some degenerated basal lamina with appearance of irregular basal unfolding and there is degeneration of some parts of the cytoplasm.

(C) Group treated with AC plus Ca/Dich showed normal appearance of the homochromatic nucleus and normal appearance of Bowman's space, collagen, red blood cells, pedicles and mesangial cell. (D) Group treated with AC plus Mg/Dich showed normal mitochondria, normal capillary lumen, normal nucleus and normal collagen. (E) Group treated with AC plus Cr/Dich showed normal capillary lumen, normal mitochondria, normal sized vacuoles, regular basal lamina, normal appearance of collagen, normal red blood cells, mesangial cell, pedicles with normal pedicles nucleus and regular nucleus membrane and normal Bowman's space with distended microvilli.

Histopathology evaluation: Photomicrographs of (A) Control group showed normal hepatic structures with normal central vein. B1-B2 AC treated group showed markedly dilated central vein filled with red blood cells lies at the center of the lobule surrounded by necrotic hepatocytes. C, D and E Groups treated with AC and then treatment with either Ca/Dich and/or Mg/Dich and/or Cr/Dich, all these groups showed normal hepatic structures with normal central vein and normal hepatic lobules. Histological activity index (HAI) was assessed based on the degree of microscopic lesions in hepatic tissues as recorded in table 8.

Histopathological examination in the kidney of rats treated groups A: Cross section of rat kidney of control group showed normal renal tubules and normal sized glomeruli. B (B1 and B2): Cross section of rat kidney treated with AC showed hypercellular glomeruli with mesangial cell proliferation with few scattered congested blood vessels with dense aggregates of chronic non-specific inflammatory cells mainly lymphoplasmacytic wit Focal glomerulosclerosis with mild tubular hemorrhage with appearance of interstitial hemorrhage.

C: Cross section of rat kidney treated with AC and Ca/Dich showing normal appearance of renal tubules and normal sized glomeruli. D: Cross section of rat kidney treated with AC and Mg/Dich showing normal appearance of kidney glomeruli and normal renal tubules. E: AC+Cr/Dich treated group showing normal appearance of renal tubules with normal two sized glomeruli. Histological activity index (HAI) was assessed based on the degree of microscopic lesions in renal tissues as recorded in table 9.

Comet assay: Comet images of cells derived from the hepatic tissues of (A) control group showed intact nuclei. (B) AC treated group showing a high percent of apoptosis by high percent of tall shadow of nuclei. (C, D and E) Groups treated with AC with either Ca/Dich, Mg/Dich and Cr/Dich, each group showed more percent of intact nuclei without any comet or tail shadow as shown in fig. 14 and the percentages of tail length and DNA damage percentage were shown in table 10.

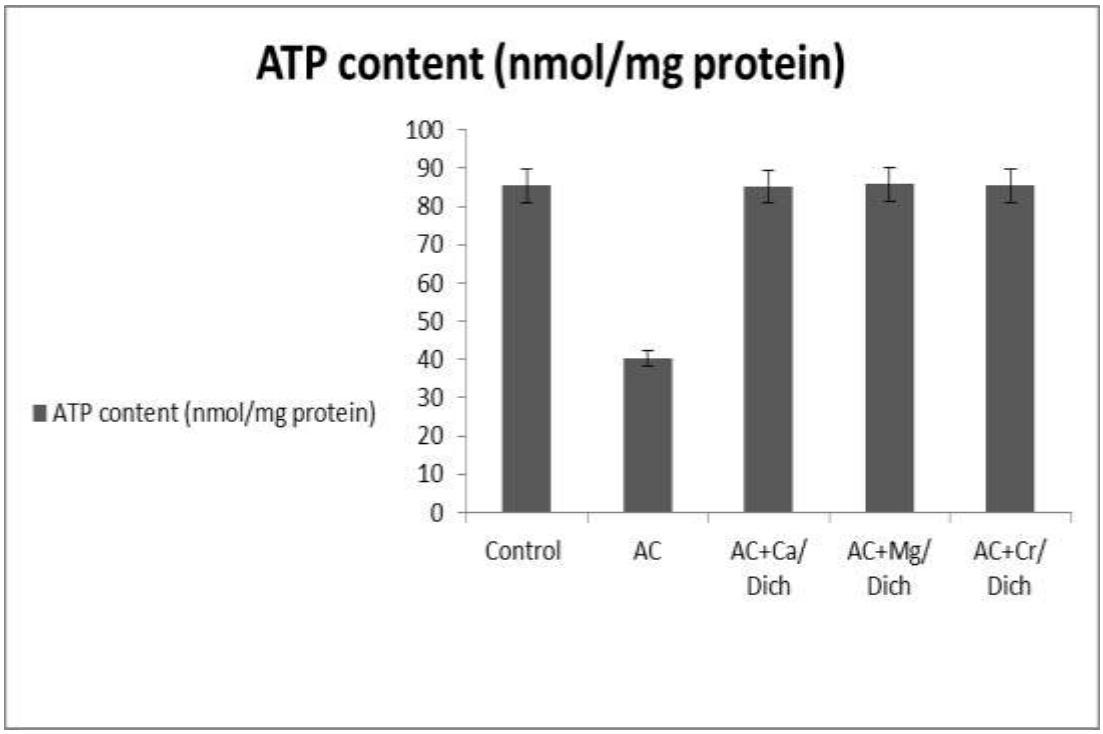

Fig. 9: The efficacy of Ca/Dich, Mg/Dich and Cr/Dich against ATP content in the rat model of nephrotoxicity and hepatotoxicity induced by Acrylamide (AC)

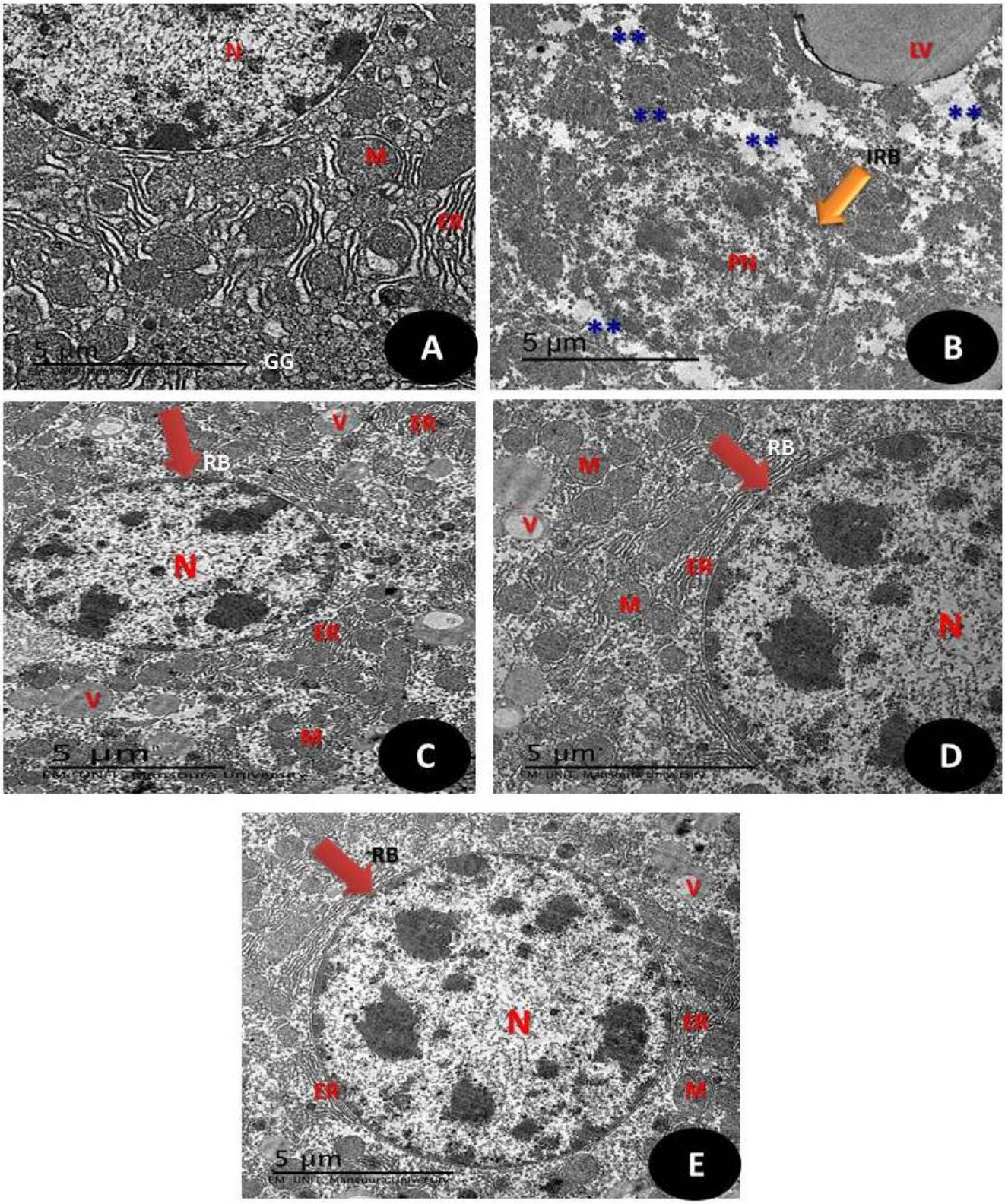

Fig. 10: Electron micrograph of liver section, (A) Control group showing the normal hepatocytes with normal nuclei (N) and normal sized mitochondria (M) and normal endoplasmic reticulum (ER) with appearance of normal glycogen granules (GG) (5µm). (B) AC treated group showed pyknotic nuclei (DN) with irregular nuclear boundaries (Orange arrow) (IRB) and disintegration of most hepatic structures (**) with severe fatty change and appearance of large vacuoles (LV) (5µm).(C , D and E) AC treated groups with either Ca/Dich ,Mg/Dich and/or Cr/Dich had normal appearance of hepatic structures with normal rounded nucleus (N) ,Regular nuclear bounderies (RB) (Red arrow), normal mitochondria (M) and normal endoplasmic reticulum (ER) with normal sized vacuoles in the cytoplasm (5µm)

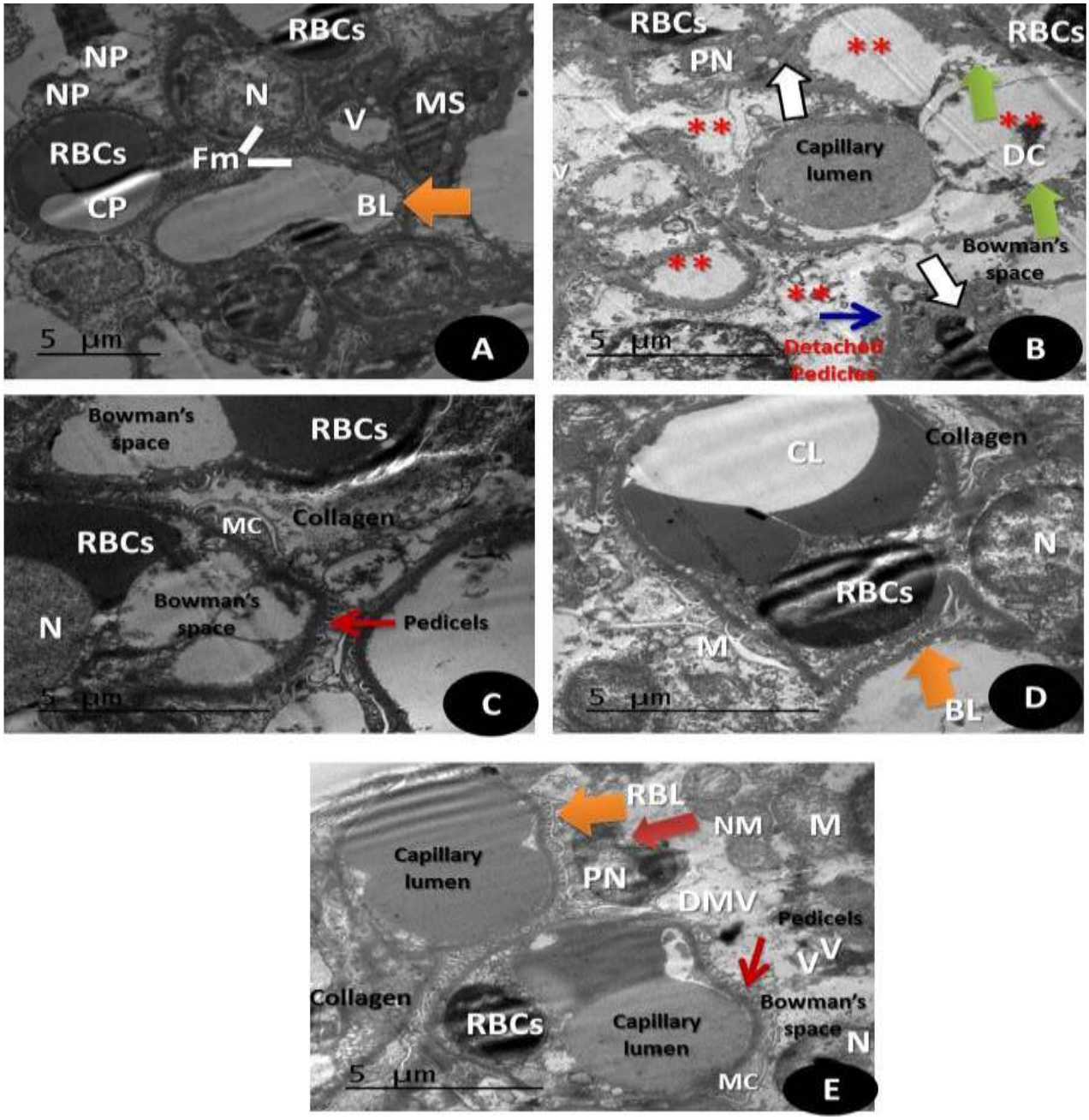

Fig. 11: Electron micrograph of kidney section, (A) Control group showing normal homogenous chromatin nucleus (N), vacuoles (v), filtration membrane (Fm), nucleus of podocyte (NP) with expansion of mesangial substance, basal lamina (BL)(Orange arrow), capillary lumen (CP), Red blood cells (RBCs). (Scale bar=5 µm) (B) Electron micrograph of kidney section of the group treated with AC showing detached pedicles (Blue arrow), disintegration of most of renal tissues (**), appearance of enlarged capillary lumen, with enlarged Bowman's space , appearance of pyknotic nuclei (PN) with disintegrated chromatin (DC), presence of excessive red blood cells (RBC), appearance of thick basal lamina (White arrow) with appearance of some degenerated basal lamina (Orange arrow), with appearance of irregular basal unfolding and there is degeneration of some parts of the cytoplasm. (Scale bar=5 µm) (C) Electron micrograph of kidney section of group treated with AC and then accompanied by Ca/Dich showed normal appearance of the homochromatic nucleus (N) and normal appearance of Bowman's space , collagen ,red blood cells (RBCs) , pedicles (red arrow) and mesangial cell (MC) (Scale bar=5 µm). (D) Electron micrograph of kidney section of group treated with AC and then accompanied by Mg/Dich showing normal mitochondria (M) , normal capillary lumen (CL), normal nucleus (N) and normal collagen. (Scale bar=5 µm) (E) Electron micrograph of kidney section of group treated with AC and then accompanied by Cr/Dich showing normal capillary lumen , normal mitochondria (M) , normal sized vacuoles (V) ,regular basal lamina (RBL), normal appearance of collagen , normal red blood cells (RBCs), mesangial cell (MC),pedicles (Red arrow) with normal pedicles nucleus (PN) and regular nucleus membrane (NM) and normal Bowman's space with distended microvilli (DMV) (Scale bar=5 µm)

Mitochondrial membrane potential: The fluorescent detection of mitochondrial membrane potential showed high improvement on the hepatic tissues treated groups (A, C ,D and E) control group or treated groups with either Ca/Dich , Mg/Dich and Cr/Dich showing non-accumulation of ROS in mitochondrial (50.0 µm). (B) AC treated group showed high accumulation of ROS in the mitochondria Because ROS accumulation is a hallmark of oxidative cell death (50.0 µm) (Fig. 15).

Effect on expressions of TNF-α and IL-6 at mRNA expression levels: The inflammatory cytokines production was evaluated by RT-PCR. The TNF-α and IL-6 mRNA levels were up-regulated in the hepatic tissues in groups treated with the novel complexes Ca/Dich, Mg/Dich and Cr/Dich compared with control untreated group (Fig.16). The complexes Ca/Dich, Mg/Dich and Cr/Dich caused a marked decrement in IL-6 and TNF-α mRNA levels (Fig. 16).

Table 8

Histological activity index (HAI) was assessed based on the degree of microscopic lesions in hepatic tissues as the effect of AC, Acrylamide; Ca/Dich, Ca/2,6-Dichloroindophenol; Mg/Dich, Mg/2,6-Dichloroindophenol; and Cr/ Dich, Cr/2,6-Dichloroindophenol separately or in combination in male rats.

Findings	Groups				
	Control	AC	AC+ Ca/ Dich	AC+ Mg/ Dich	AC+ Cr/ Dich
Normal hepatic structures	++++	------	++++	++++	++++
Dilated central vein	------	++++	------	------	------
Necrotic hepatocytes	------	++++	------	------	------
Fibrosis	------	++++	------	------	------
Mild congested central vein	------	++++	------	------	------
Severe congested central vein	------	++++	------	------	------

– no found; ---+ found in 1–3 rats; ++-- found in 4–6 rats; +++- found in 6–7 rats , ++++ found in 7-8 rats at least.

Table 9

Histological activity index (HAI) was assessed based on the degree of microscopic lesions in renal tissues as the effect of AC, Acrylamide ; Ca/Dich, Ca/2,6-Dichloroindophenol; Mg/Dich, Mg/2,6-Dichloroindophenol; and Cr/ Dich, Cr/2,6-Dichloroindophenol.separately or in combination in male rats.

Findings	Groups				
	Control	AC	AC+ Ca/Dich	AC+ Mg/Dich	AC+ Cr/Dich
Normal renal tubules (T)	++++	------	++++	++++	++++
Normal sized glomeruli (G)	++++	------	++++	++++	++++
Hypercellular glomeruli with mesangial cell proliferation	------	++++	------	------	------
Interstitial hemorrhage	------	++++	------	------	------
Mild tubular hemorrhage	------	++++	------	------	------
Congested blood vessels	------	++++	------	------	------

– no found; ---+ found in 1–3 rats; ++-- found in 4–6 rats; +++- found in 6–7 rats, ++++ found in 7-8 rats at least.

Table 10

The protective effect of AC, Acrylamide; Ca/ Dich, Ca/2,6-Dichloroindophenol; Mg/Dich, Mg/2,6-Dichloroindophenol; and Cr/ Dich, Cr/2,6-Dichloroindophenol against oxidative DNA damage in the liver (tail length, DNA% and tail moment) and apoptotic cell population (apoptosis %) induced by AC.

Group	Tail Length (px)	DNA in Tail %	Tail Moment (Units)	Apoptosis %
Control	3.30 ± 0.58^{c}	2.77 ± 0.36^{bc}	0.36 ± 0.05^{bc}	8.63 ± 1.51^{c}
AC	10.47 ± 1.02^{a}	20.96 ± 2.65^{a}	4.55 ± 0.81^{a}	83.04 ± 5.25^{a}
AC+ Ca/ Dich	3.33 ± 0.25^{c}	2.22 ± 0.03^{c}	0.30 ± 0.01^{c}	8.86 ± 1.10^{c}
AC+ Mg/ Dich	3.35 ± 0.49^{c}	2.40 ± 0.03^{c}	0.39 ± 0.10^{bc}	8.76 ± 1.15^{c}
AC+ Cr/ Dich	3.51 ± 0.28^{bc}	2.37 ± 0.15^{c}	0.32 ± 0.10^{c}	8.60 ± 1.00^{c}

AC, Acrylamide; Ca/ Dich, Ca/2,6-Dichloroindophenol; Mg/ Dich, Mg/2,6-Dichloroindophenol; and Cr/ Dich, Cr/2,6-Dichloroindophenol**.** Values are expressed as means ±SE; n = 10 for each treatment group. Symbols are arranged alphabetically indicate significance comparison as compared to control group and other treated groups from higher to lower ($p< 0.05$).

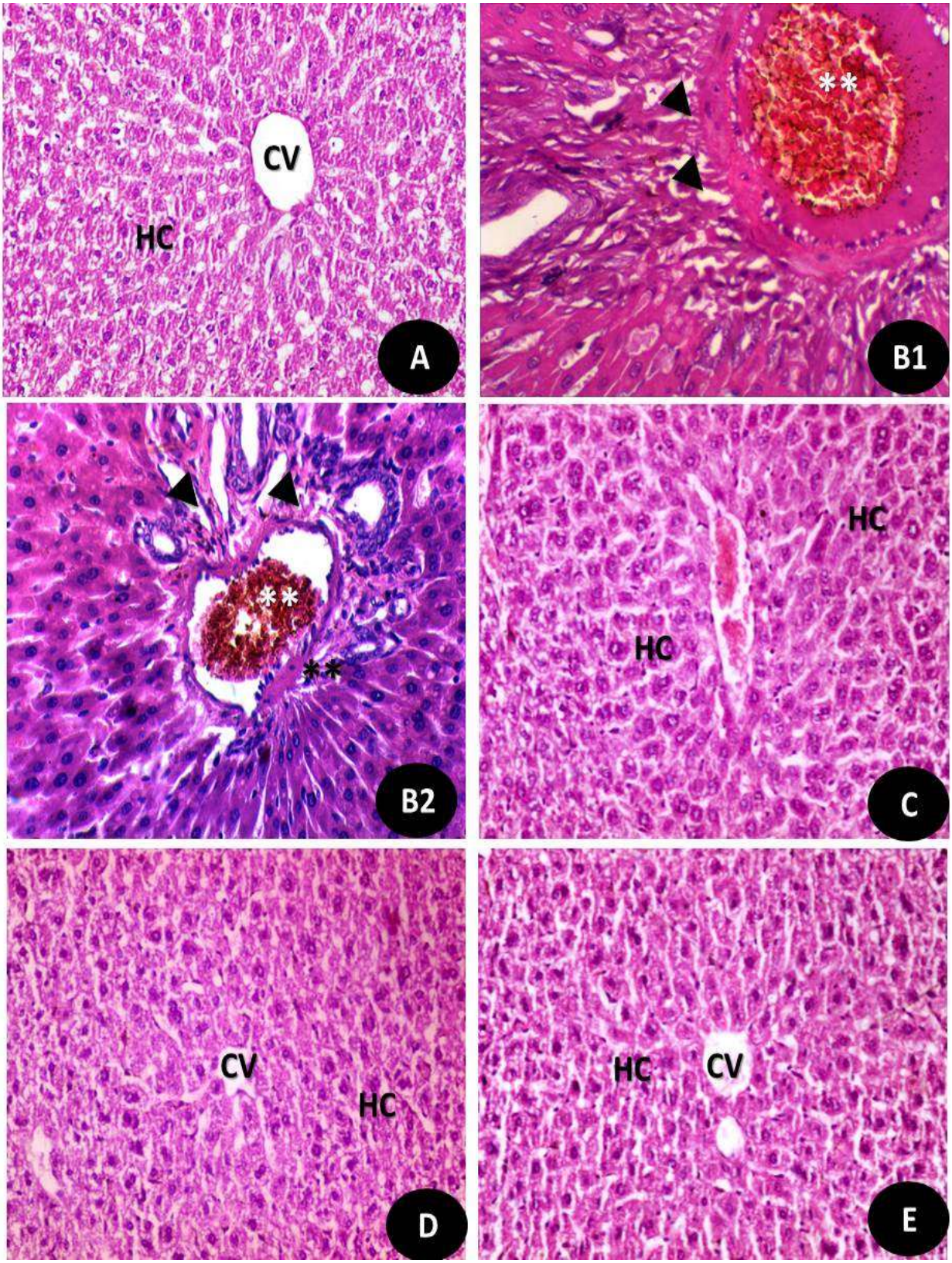

Fig. 12: Photomicrographs of (A) Control group: showing normal hepatic structures (HC) with normal central vein (CV) (X400). (B1-B2) AC treated group showed markedly dilated central vein (CV) filled with red blood cells (White asterisk **)lies at the center of the lobule surrounded by the hepatocytes pericentral zone shows necrotic hepatocytes (**) with portocentral fibrosis (Black head arrow) with infiltration with lymphocytes (*) lies at the center of the lobule s (X400).(C,D and E) Groups treated with AC and then treatment with either Ca/Dich and/or Mg/Dich and/or Cr/Dich, all these groups showed normal hepatic structures (HC) with normal central vein (CV) and normal hepatic lobules (X400)

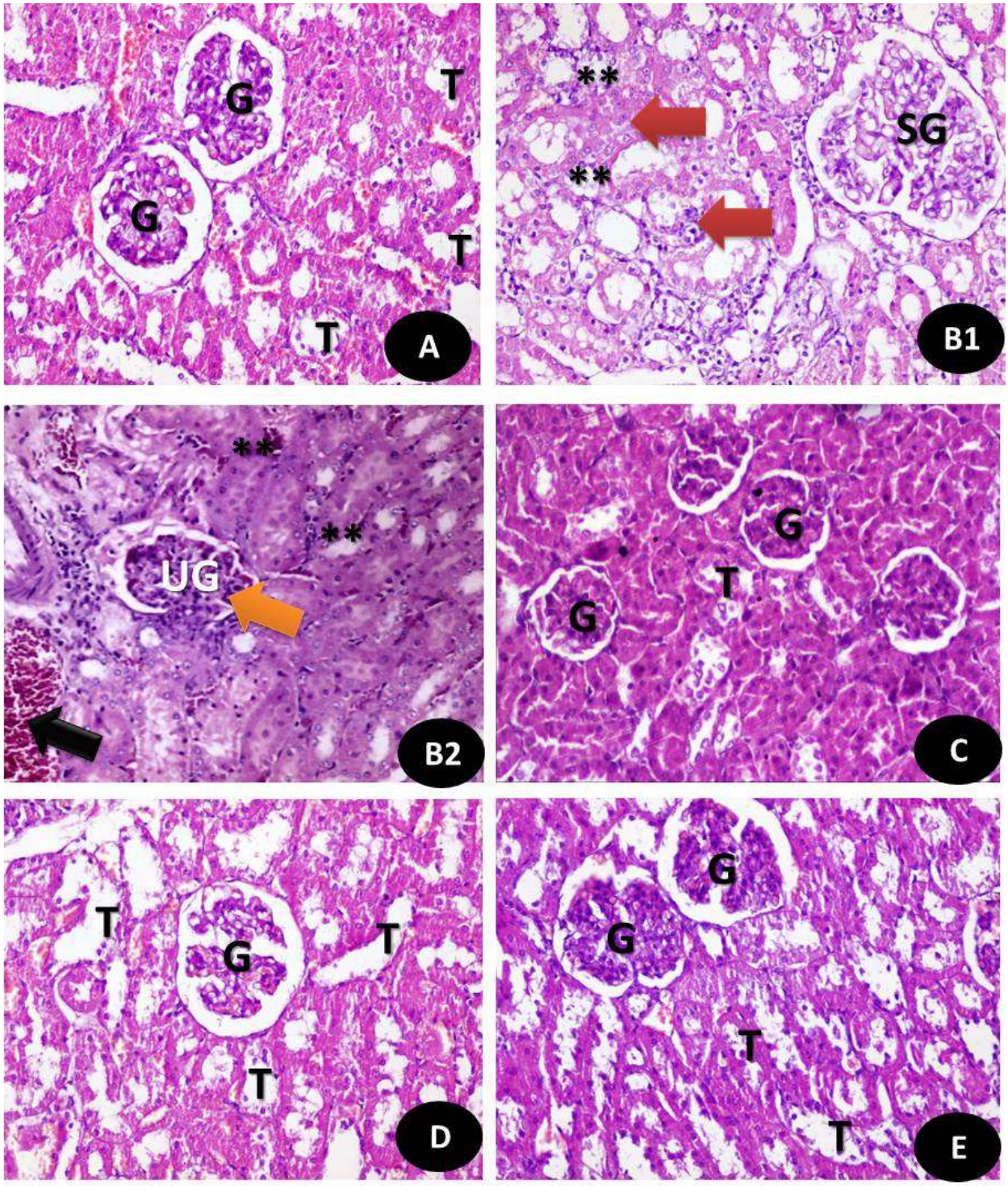

Fig. 13: Histopathological examination in the kidney of rats treated groups (H &E). A: Cross section of rat kidney of control group showing normal renal tubules (T) and normal sized glomeruli (G) (x400). B (B1 and B2): Cross section of rat kidney treated with AC showing hypercellular glomeruli with mesangial cell proliferation (SG) with few scattered congested blood vessels (**) with dense aggregates of chronic non-specific inflammatory cells mainly lymphoplasmacytic (red arrow) Focal glomerulosclerosis with mild tubular hemorrhage (UG) (Orange arrow) with appearance of interstitial hemorrhage (Black arrow) (X400). C: Cross section of rat kidney treated with AC and Ca/Dich showing normal appearance of renal tubules (T) and normal sized glomeruli (G). (X400). D: Cross section of rat kidney treated with AC and Mg/Dich showing normal appearance of kidney glomeruli (G) and normal renal tubules (T) (X400). E: AC+Cr/Dich treated group showing normal appearance of renal tubules (T) with normal two sized glomeruli (G). (X400)

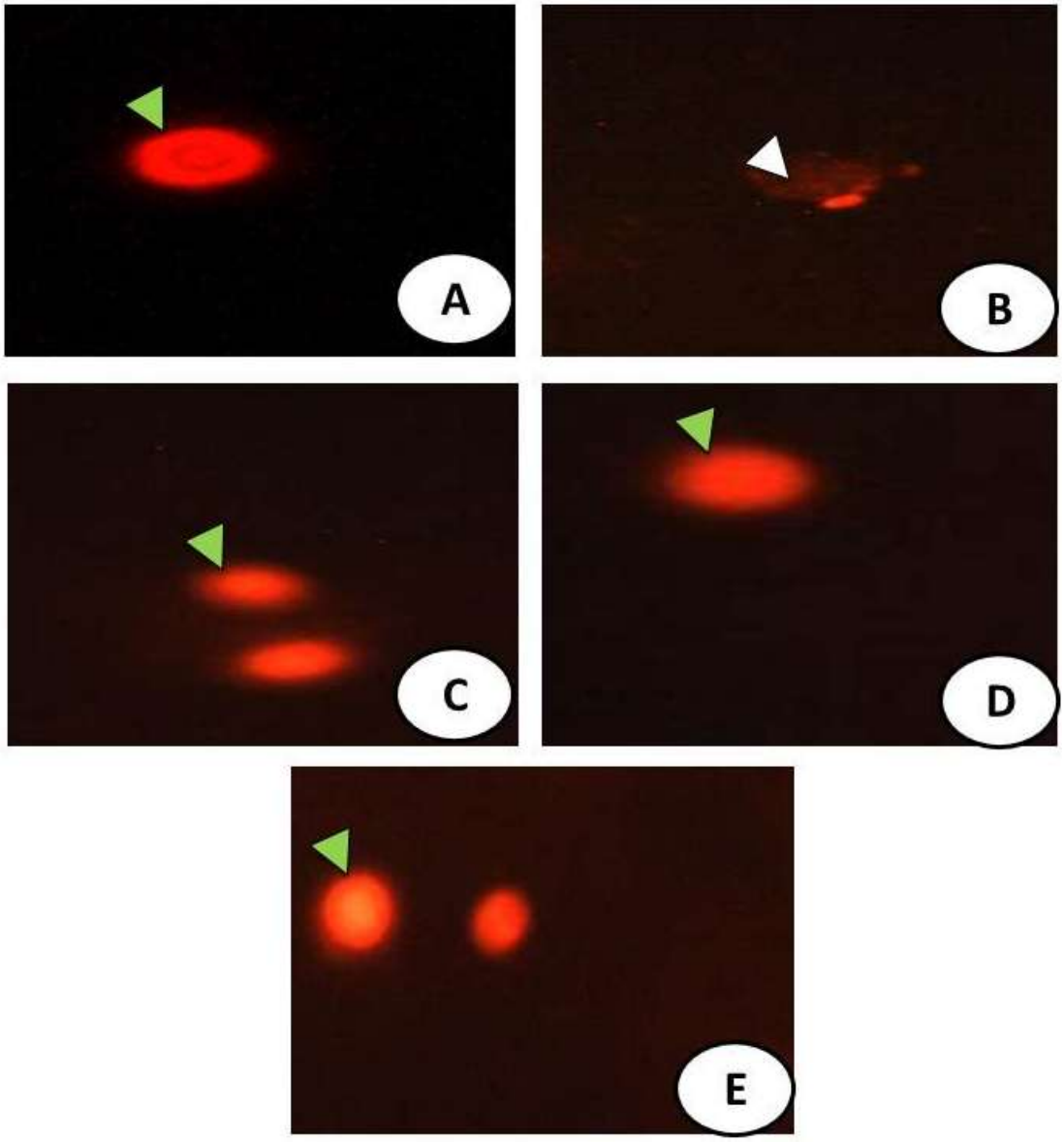

Fig. 14: Comet images of cells derived from the hepatic tissues of (A) control group which showed intact nuclei. (B) AC treated group showing a high percent of apoptosis by high percent of tall shadow of nuclei. (C, D and E) Groups treated with AC with either Ca/Dich , Mg/Dich and Cr/Dich , each group showed more percent of intact nuclei without any comet or tail shadow

Discussion

The current study is a considered as a new strategy for serving hepatorenal protection against hepatic damage and injury induced by AC by using new complexity between 2,6 dichlorobenzeyne indophenol with Ca , Mg and Cr metals which will open new gate for the excellence in the protection of liver and kidney from sever inflammation like COVID-19 and can alleviate viral toxicity and protect the body vital organs.

Dich/Sr, Dich/Ba and Dich/Fe treatment induced hepatorenal protection that was clarified by declining high hepatic enzymes that was elevated by AC, declining tumor markers and inflammatory markers like interleukin-6, enhancing mitochondrial potential and improving liver and kidney histological and ultrastructural sections.

Histopathological examination of liver sections of Dich-treated rats showed hepatocellular hypertrophy and anisocytosis. These results were similar to those seen with other chlorobenzene isomers (penta- and hexa-) that have been studied[49]. The obtained results confirmed the vital role of the novel complexes Ca/Dich, Mg/Dich and Cr/Dich that greatly succeeded in alleviating the hepatic and renal toxicity induced by AC. Dich alone induced severe damages by appearance of nodules and dark black spots with rupture of most of hepatic structures as appeared in TEM and histological sections.

Dich had no effect on promoting GST level[49]. This is in contrast to the current finding who confirmed the high protective effect of novel complexes/Dich, (Ca/Dich , Mg/Dich and Cr/Dich) which induced significant increment

in all antioxidant enzymes (SOD, CAT and GRx) with marked declining of marker of lipid peroxidation (MDA) which confirmed the high hepatotoxicity induced by the synthesized complexes and declining tumor markers and decrement of cytokine storm induced by AC.

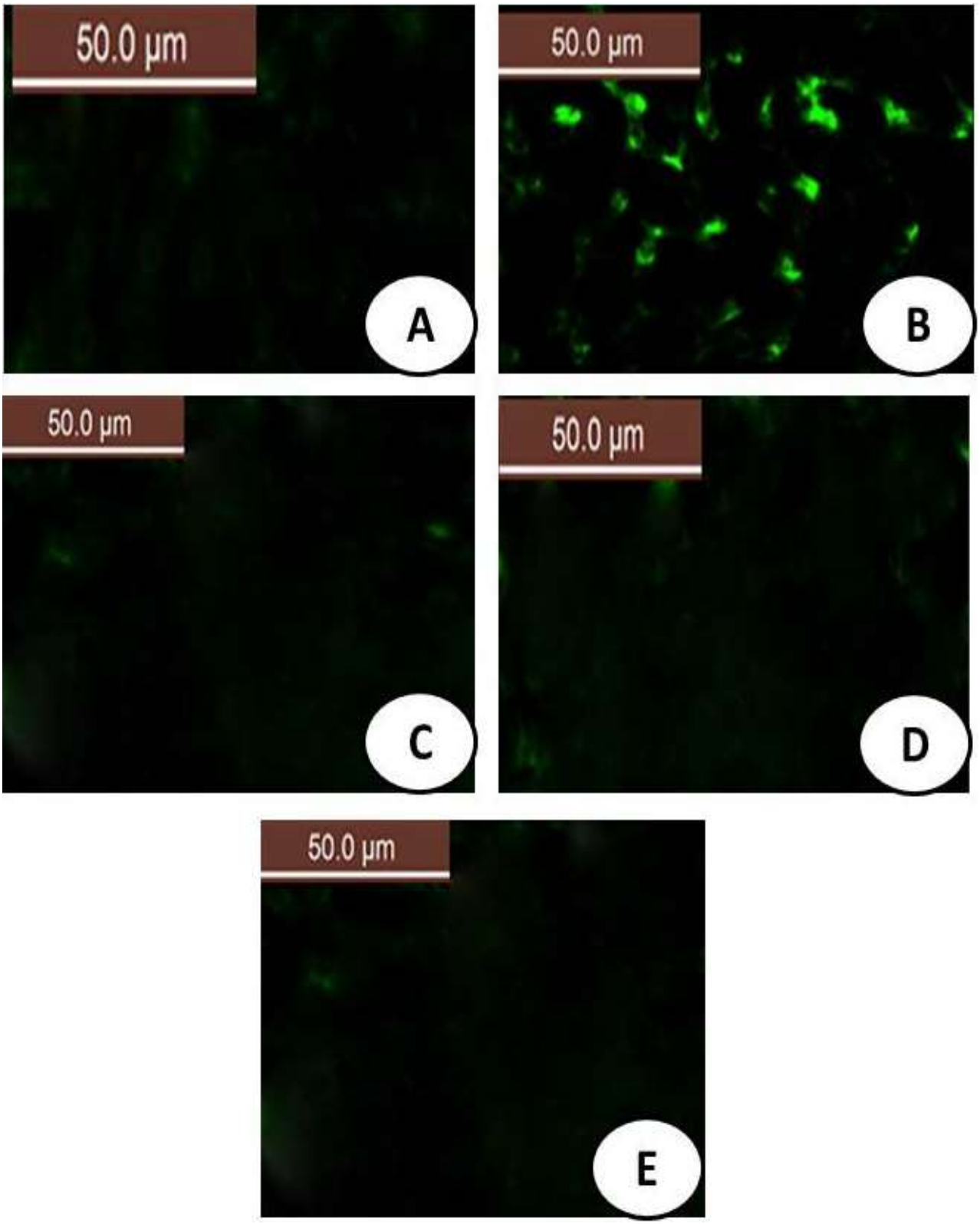

Fig. 15: The fluorescent detection of mitochondrial membrane potential showed high improvement on the hepatic tissues treated groups (A, C ,D and E) control group and other treated groups with AC and combined with either Ca/Dich, Mg/Dich and Cr/Dich showing non-accumulation of ROS in mitochondrial membrane (50.0 µm). (B) AC treated group showing high accumulation of ROS in the mitochondria Because ROS accumulation is a hallmark of oxidative cell death (50.0 µm)

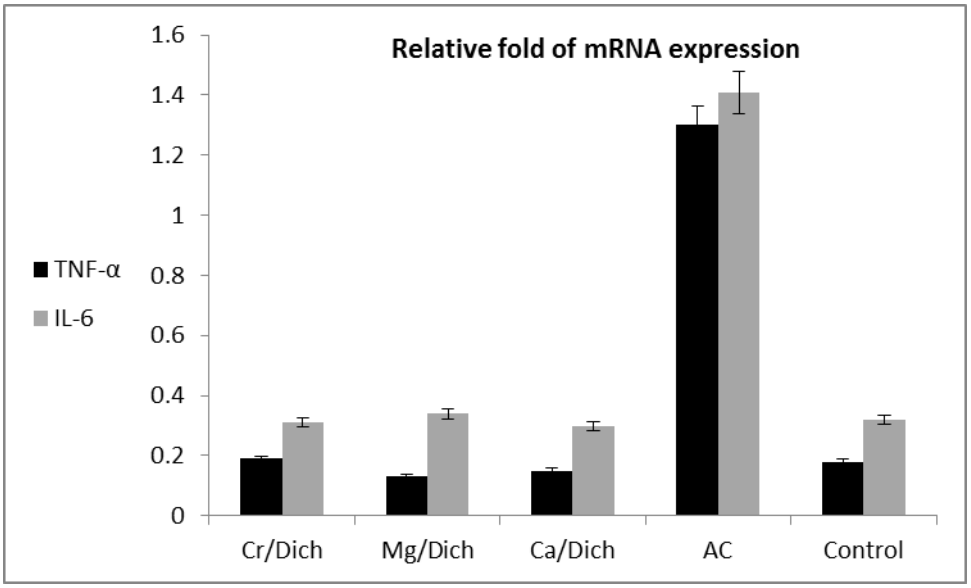

Fig. 16: Relative fold of mRNA expression of IL-6 and TNF-α in treated groups.

AC induced severe hepatic damages represented by high hepatic enzyme levels (AST and ALT) and declined cellular antioxidant enzymes and elevate marker of lipid peroxidation (MDA) beside induction of hepatic histological damages and congestion of the central vein and fibrosis beside hepatic ultrastructural alterations as confirmed in the current study and all these structural changes were alleviated by the novel complexes (Ca/Dich, Mg/Dich and Cr/Dich) who greatly improved hepatic structures and restored biomarkers of liver and kidney to about normal levels with improving histological and ultrastructural examination and this confirmed the concept of the current study by the ability of the novel complexes to act as hepatoprotectant and renal protective agents against AC toxicity and this would be beneficial in alleviating COVID-19 toxicity.

Chromium(III) is considered as essential trace element in the human body which plays a crucial role in the biochemistry of all the living organisms[11]. This is greatly reinforced in the current study by the hepatorenal protective activity of Cr/Dich in protection against liver and kidney damages and improving histological and ultrastructural of these vital organs and this may be attributed to the role of Cr in restoring normal structures of the liver and kidney after treatment with AC and also may interact with 2,6-dichloroindophenol and give new protective formula against oxidative injury and genotoxicity.

Dabak et al[10] previously confirmed the great role of Ca and Mg metals as hepatoprotective agent against lead and cadmium toxicity. This clarifies the great role of the nutrients in controlling internal body environment and also confirms our concept by its role as protective agent after complexation of Ca and Mg with 2,6-Dichloroindophenol.

Conclusion

Alanine and aspartate aminotransferase activities mostly depend on hepatotoxicity biomarkers. ALT is a hepatic enzyme that plays a vital role in amino acid metabolism and glucose genesis and genolysis. ALT normal levels are within in the range of 5-50 U/L. Elevated level of this hepatic enzyme is released during liver injury[1] which is greatly confirmed by the results of the current study and confirming the protective role of the novel synthesized complexes (Ca/Dich, Mg/Dich and Cr/Dich).

ALT estimation is a more specific test for detecting hepatic tissue abnormalities since it is 1rly found in the liver[1]. However, lower enzymatic activities are also found in the skeletal and cardiac muscles. This enzyme is responsible for detection of the hepatocellular necrosis. These finding are greatly confirmed by the current finding which revealed elevation of ALT n AC treated group and declining of this level in AC accompanied by treatment with the novel complexes (Ca/Dich, Mg/Dich and Cr/Dich) and this confirms the role of the novel complexes in alleviating AC toxicity.

Acknowledgement

This work was supported by grants from Deanship of Scientific Research, Taif University, Saudi Arabia under Research Group project Grants No. 6144-440-1.

References

1. Singh Anita, Bhat Tej K. and Sharma Om P., Clinical Biochemistry of Hepatotoxicity, *J Clinic Toxicol*, **S4**, 001 **(2011)**

2. Willett K.L., Roth R.A. and Walker L., Workshop overview: hepatotoxicity assessment for botanical dietary supplements, *Toxicol Sci*, **79**, 4-9 **(2004)**

3. Papay J.I. et al, Drug-induced liver injury following positive drug rechallenge, *Regul Toxicol Pharmacol*, **54**, 84-90 **(2009)**

4. Saukkonen J.J. et al, An Official ATS Statement: Hepatotoxicity of antituberculosis therapy, *Am J Respir Crit Care Med*, **174**, 935-952 **(2006)**

5. Deng X., Luyendyk J.P., Ganey P.E. and Roth R.A., Inflammatory stress and idiosyncratic hepatotoxicity: Hints from animal models, *Pharmacol Rev*, **61**, 262-282 **(2009)**

6. Kedderis G.L., Biochemical basis of hepatocellular injury, *Toxicol Pathol*, **24**, 77-83 **(1996)**

7. Bleibel W., Kim S., D'Silva K. and Lemmer E.R., Drug-induced liver injury: Review Article, *Dig Dis Sci*, **52**, 2463-2471 **(2007)**

8. Chang C.Y. and Schaino T.D., Review article: Drug hepatotoxicity, *Aliment Pharmacol Ther*, **25,** 1135-1151 **(2007)**

9. Naruse K., Tang W. and Makuuchi M., Artificial and bioartificial liver support: A review of perfusion treatment for hepatic failure patients, *World J Gastroenterol*, **13**, 1516-1521 **(2007)**

10. Dabak J.D., Gazuwa S.Y. and Ubom G.A., Hepatoprotective potential of calcium and Magnesium against cadmium and lead induced Hepatotoxicity in Wistar rats, *Asian Journal of Biotechnology*, **1(1),** 12-19 **(2009)**

11. Sylwia Terpiłowska and Andrzej Krzysztof Siwicki, Chromium(III) and iron(III) inhibits replication of DNA and RNA viruses, *Biometals*, **30**, 565–574 **(2017)**

12. Hamza Reham Z., EL-Megharbel Samy M., Altalhi Tariq, Gobouri Adil A. and Alrogi Ashjan Ayad, Hypolipidemic and hepatoprotective synergistic effects of selenium nanoparticles and vitamin. E against acrylamide induced hepatic alterations in male albino mice, *Appl Organometal Chem*., **34**, e5458 **(2020)**

13. Gunawardhana L., Mobley S.A. and Sipes I.G., Modulation of 1,2- Dichlorobenzene hepatotoxicity in the Fischer- 344 rat by scavenger of superoxide Anions and an inhibitor of kupffer cells, *Toxicology and Applied Pharmacology*, **119,** 205-213 **(1993)**

14. Ohkawa H., Ohishi N. and Yagi K., Assay for lipid peroxides in animal tissues by thiobarbituric acid reaction, *Anal Biochem*., **95**, 351-8 **(1970)**

15. Marklund S. and Marklund G., Involvement of the superoxide anion radical in the autoxidation of pyrogallol and a convenient assay for superoxide dismutase, *Europ. J. Biochem*., **47**, 469–474 **(1974)**

16. Aebi H., Catalase in vitro, *Meth. Enzymol.*, **105**, 121 –126 **(1984)**

17. Couri D. and Abdel-Rahman M.S., Effect of chlorine dioxide and metabolites on glutathione-dependent system in rat, mouse and chicken blood, *J. Environ. Pathol. Toxicol*., **3**, 451–460 **(1980)**

18. Hafeman D.G., Sunde R.A. and Hoekstra W.G., Effect of dietary selenium on erythrocyte and liver glutathione peroxidase in the rat, *J. Nutrit*., **104**, 580–587 **(1974)**

19. Suzuki K., Ota H., Sasagawa S., Sakatani T. and Fujikura T., Assay method for myeloperoxidase in human polymorphonuclear leukocytes, *Anal Biochem*., **132**, 345–352 **(1983)**

20. Litwack G., Bothwell J.W., Williams J.N. and Elvehjem C.A., A colorimetric assay for xanthine oxide in rat liver homogenates, *J. Biol. Chem*., **200**, 303–310 **(1953)**

21. Hu M.L., Measurement of protein thiol groups and glutathione in plasma, *Methods Enzymol*., **233**, 380–5 **(1994)**

22. Carr T., Andressen C.J. and Rudel L.L., Enzymatic determination of triglyceride, free cholesterol and total cholesterol in tissue lipid extracts, *Clin Chem*., **26**, 39–42 **(1993)**

23. Warnick G.R., Benderson J. and Albers J.J., Selected methods of clinical chemistry, *Amer Assoc. Clin. Chem*., **10**, 91–9 **(1983)**

24. Friedewald W.T., Estimation of concentration of low-density lipoprotein cholesterol in plasma without use of the preparative ultracentrifuge, *Clin. Chem*., **18**, 499–502 **(1972)**

25. Bradford M.M., A Rapid and Sensitive Method for the Quantitation of Microgram Quantities of Protein Utilizing the Principle of Protein-Dye Binding, *Analytical Biochemistry*, **72**, 248-254 **(1976)**

26. Reitman S. and Frankel S., A colorimetric method for the determination of serum glutamic oxaloacetic and glutamic transaminase, *Amer. J. Clin. Pathology*, **28**, 56 **(1957)**

27. Young D.C., Koon H.R. and Hyung K.C., In vitro and in vivo experimental effect of Korean red ginseng on erection, *The Journal of Urology*, **162**, 1508-1511 **(1999)**

28. Vassault A., Lactate dehydrogenase, UV-method with pyruvate and NADH, in Bergmeyer J. and Grabl M., eds., Methods of Enzymatic Analysis, Verlag-Chemie, Deerfield Beach, Florida, 119–126 **(1983)**

29. Schirmeister J.H., Willmann and Kiefer H., Critical evaluation of plasma cretinine as attest of glomerulus filtrate, *Verhandlungen Deutschen Gesellschaft Innere Med*., **70**, 678-681 **(1964)**

30. Fossati P., Prencipe L. and Berti G., Use of 3,5-dichloro-2-hydroxybenzenesulfonic acid/4-aminophenazone chromogenic system in direct enzymic assay of uric acid in serum and urine, *Clin. Chem*., **26**, 227-231 **(1980)**

31. Patton C.J. and Crouch S.R., Spectrophotometric and kinetics investigation of the Berthelot reaction for the determination of ammonia, *Anal. Chem*., **49**, 464-469 **1977**

32. Wener M.H., Daum P.R. and McQuillin G.M., The influence of age, sex and race on the upper reference limit of serum C-reactive protein concentration, *J Rheumatol.*, **27(10),** 2351-2359 **(2000)**

33. Zhao Y. et al, Vanadium compounds induced mitochondria permeability transition pore (PTP) opening related to oxidative stress, *J Inorg Biochem.*, **104**, 371-8 **(2010)**

34. Ayoubi M. et al, Biochemical mechanisms of dose-dependent cytotoxicity and ROS-mediated apoptosis induced by lead sulfide/graphene oxide quantum dots for potential bioimaging applications, *Sci Rep*., **7**, 12896 **(2017)**

35. Naserzadeh P. et al, Single-walled carbon nanotube, multiwalled carbon nanotube and Fe2O3 nanoparticles induced mitochondria-mediated apoptosis in melanoma cells, *Cutan Ocul Toxicol*., **37**, 157-66 **(2018)**

36. Tafreshi N., Hosseinkhani S., Sadeghizadeh M., Sadeghi M., Ranjbar B. and Naderi-Manesh H., The influence of insertion of a critical residue (Arg356) in structure and bioluminescence spectra of firefly luciferase, *J Biol Chem*., **282**, 8641-7 **(2007)**

37. Gabe M., Techniques histologiques [Histological Techniques], Paris, Masson Publisher **(1968)**

38. Weakley B. and Beginner S., Handbook in Biological Transmission Electron Microscopy, Second edition, Churchill Livingstone, London **(1981)**

39. Endoh D., Okui T., Ozawa S., Yamato O., Kon Y., Arikawa J. and Hayashi M., Protective effect of a lignan-containing flaxseed extract against CCl (4)-induced hepatic injury, *J Vet Med Sci*., **64(9),** 761-5 **(2002)**

40. Collins A.R. and Dunsinka M., Oxidation of cellular DNA measured with the comet assay, In Armstrong D., eds., Methods in Molecular Biology: Oxidative stress Biomarkers and antioxidant Protocols, Humana Press, New Jersey, 147-159 **(2002)**

41. Geary W.J., The Use of Conductivity Measurements in Organic Solvents for the Characterisation of Coordination Compounds, *Coord. Chem. Rev.*, **7**, 81 **(1971)**

42. Nakamoto K., Infrared and Raman Spectra of Inorganic and Coordination Compounds, Wiley, New York **(1986)**

43. Thomas M., Nair M.K.M. and Radhakrishnan P.K, Rare Earth Iodide Complexes of 4-(2′,4′-Dihydroxyphenylazo) Antipyrine, *Synth. React. Inorg. Met. Org. Chem*., **25**, 471 **(1995)**

44. Bellamy L.J., The Infrared Spectra of Complex Molecules, second edition, Chapman & Hall, Methuen, London **(1958)**

45. Yohannan Panicker C., Tresa Varghese H. and Philip D., FT-IR, FT-Raman and SERS spectra of vitamin C, *Spectrochimica Acta Part A: Molecular and Biomolecular Spectroscopy*, **65(3–4),** 802–804 **(2006)**

46. Coates J., Interpretation of infrared spectra, a practical approach, In Encyclopedia of Analytical Chemistry, Meyers R.A., eds., John Wiley & Sons Ltd., Chichester, 10815–10837 **(2000)**

47. Lever A.B.P., Electronic spectra of dn ions Inorganic electronic specroscopy, 2nd edition **(1984)**

48. Cotton F.A. and Wilkinson G., The element of first transition series Advanced inorganic chemistry, 3rd edition **(1992)**

49. Gustafson Daniel L., Coulson Amy L., Feng Lixin, Pott Wendy A., Thomas Russell S., Chubb Laura S., Saghir Shakil A., Benjamin Stephen A. and Yang Raymond S.H., Use of a medium-term liver focus bioassay to assess the hepatocarcinogenicity of 1,2,4,5-tetrachlorobenzene and 1,4-dichlorobenzene, *Cancer Letters*, **129**, 39–44 **(1998)**.

(Received 31th October 2020, accepted 30th November 2020)